Electronic Supplementary Information (ESI)

Continuous Flow Synthesis of PCN-222 (MOF-545) with Controlled Size and Morphology: A Sustainable Approach for Efficient Production

Alessio Zuliani,[a]* M. Carmen Castillejos, Noureddine Khiar,[a]*

[a] Asymmetric Synthesis and Nanosystem Group (Art&Fun), Institute for Chemical Research (IIQ), CSIC-University of Seville, 41092 Sevilla, Spain

*Corresponding authors:

a.zuliani@csic.es

khiar@iiq.csic.es

Table of contents

S1. Details of the c.f. system

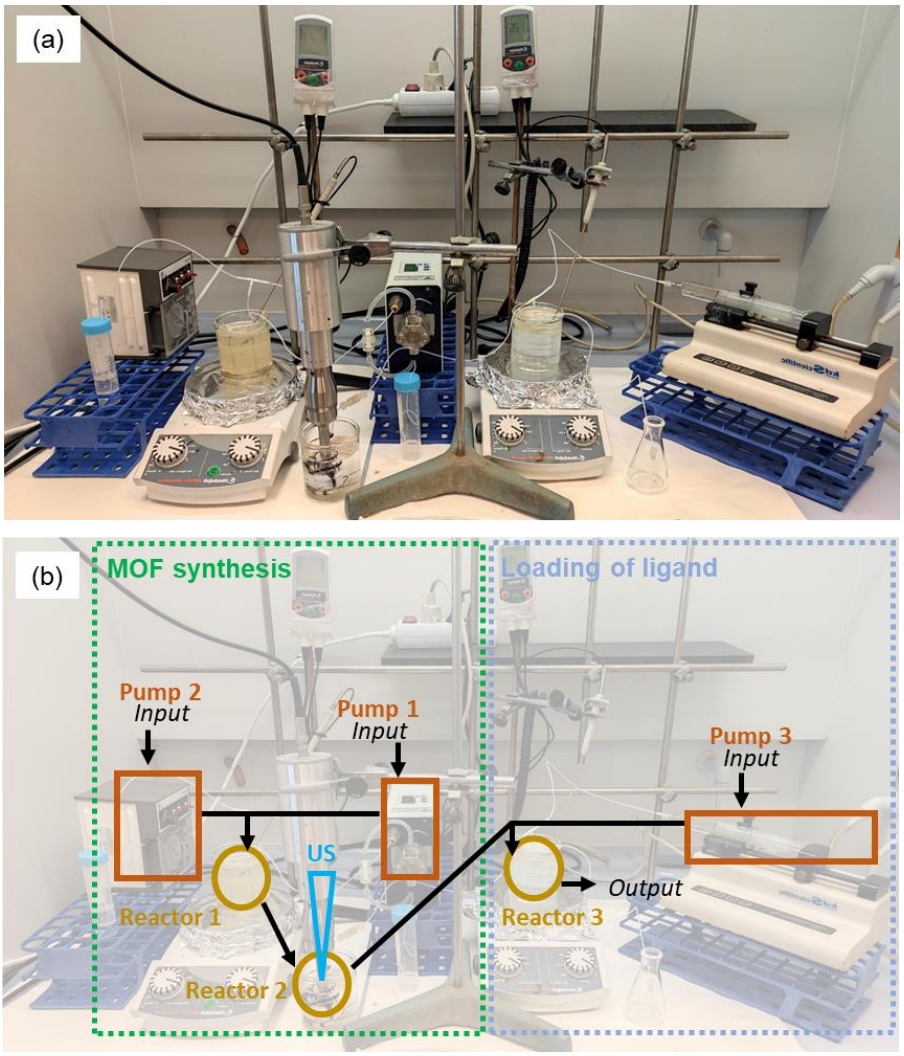

Fig. S1 (a) Picture and (b) scheme of the c.f. system.

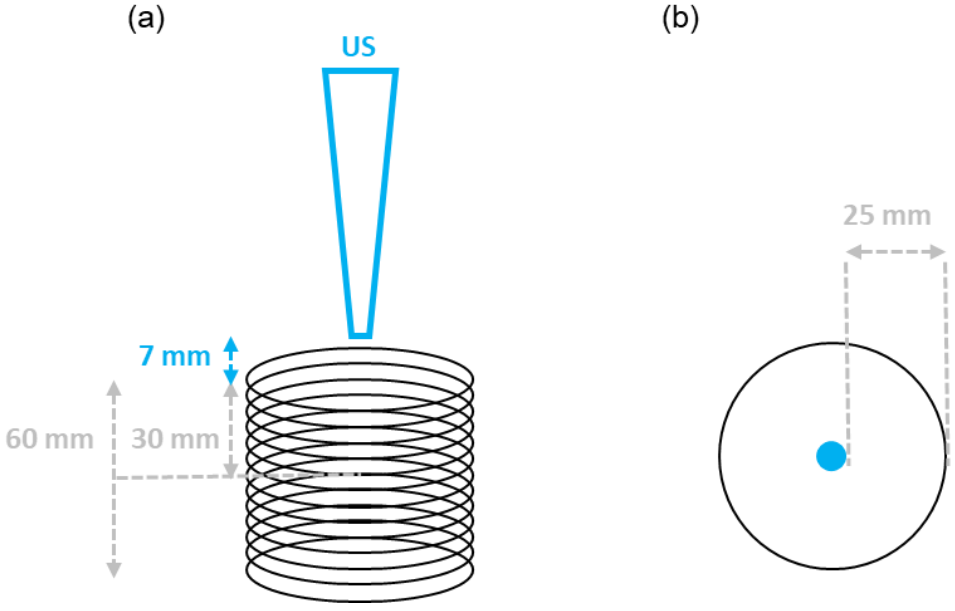

Fig. S2 Details of the position of the ultrasonic horn in Reactor 2 (a) front and (b) upper view.

S2. Materials and methods

Materials

$Zr(OBu)_4$ in n-butanol (80%$_{wt}$), benzoic acid (ACS reagent, ≥99.5%), methanol (MeOH,99.8%) isopropanol (iPrOH, natural, ≥98%), ethanol (EtOH, 96%, EMPROVE® EXPERT, Ph. Eur., BP, ChP), N,N-dimethylformamide (DMF; anhydrous, 99.8%), trifluoroacetic acid (TFA, ReagentPlus®, 99%), dimethyl sulfoxide (DMSO, ≥99%), cyclohexanone (ACS reagent, ≥99.0%), anisole (99%), dichloromethane (DCM, ≥99.8%), trichloromethane (TCM, ≥99%), toluene (99.8%), acetonitrile (CAN, 99.8%), triethylamine(≥99.5%), sodium ethoxide (95%), thionyl chloride (ReagentPlus®, ≥99%), sodium periodate (ACS reagent, ≥99.8%), Ruthenium (III) chloride trihydrate (technical grade), 2,4-Bis(4-methoxyphenyl)-2,4-dithioxo-1,3,2,4-dithiadiphosphetane (Lawesson's Reagent, 97%), 4-(dimethylamino)pyridine (DMAP, ReagentPlus®, ≥99%) and diisopropylethylamine (DIPEA, ReagentPlus®, ≥99%) were purchased from Merck KGaA (Darmstadt, Germany). Octaenglycol (≥98%) and tetrakis(4-carboxyphenyl)porphyrin (97%) were purchased from BLD Pharmatech Ltd (Shanghai, China). 2-acetamido-2-deoxy-1,3,4,6-tetra-oacetyl-β-D-galactopyranose was purchased from Biosynth (Staad, Switzerland). All the chemicals were used without any further purification.

Characterization

Scanning Electron Microscopy (SEM) images were acquired using a HITACHI S4800 field emission microscope operating at 2 kV in secondary electron and backscattered electron modes. The samples were prepared by drying a diluted dispersion of the particles on a silicon wafer substrate under ambient conditions. Dynamic Light Scattering (DLS) measurements were performed using a Malvern Zetasizer Nano ZSP equipped with a 10 mW He–Ne laser operating at a wavelength of 633 nm. Diluted samples (ca. 0.2 mg mL^{-1}) were loaded into a quartz cuvette, and then three measurements, each consisting of twelve data runs, were taken at room temperature (293 K) after an equilibration step of 10 sec. Powder X-Ray Diffraction (PXRD) analysis was conducted using a Bruker D8-Advance Diffractometer, employing X-ray radiation of Cu Kα. The measurement range spanned from 2° to 50° (2θ) with a step of 0.02°. Fourier-Transform Infrared Spectroscopy (FTIR) analysis was performed on a Bruker Tensor 27 spectrophotometer. Spectra were recorded at room temperature in the range of 400 to 4000 cm^{-1} with a resolution of 2 cm^{-1}. Dried samples were prepared on a KBr pellet. N_2 physisorption analysis involved carrying out N_2 sorption isotherms at 77 K on a Quantachrome Autosorb-iQ-2 MP/XR gas sorption analyser. Prior to analysis, the samples were degassed under vacuum at 393 K for 24 hours. Thermogravimetric analysis (TGA) of powder samples was performed using a Thermal Advantage SDT-600 instrument. The samples underwent a general heating profile from 293 K to 800 K with a heating rate of 5 $K{\cdot}min^{-1}$ under air. ^1H NMR and ^{13}C NMR spectra were recorded on a 400 MHz Bruker Avance III HD spectrometer and referenced to residual solvent. For the experiments of lectin adhesion to PCN-222@SO_3-PEG-S-GalNAc, 0.1 mL of a solution 10 mg mL^{-1} of PCN-222@ SO_3-PEG-S-GalNAc or PCN-222 was mixed with 0.3 mL of lectins labelled with FITC or AlexaFluor594 from Invitrogen™, each at a concentration of 20 μg mL^{-1}. The lectins used were ConA and PNA. After 5 minutes of incubation, the samples were collected by high-speed centrifugation (12,000 rpm, 15 min), washed three times with water, and exchanged one time with ethanol (EtOH). Finally, each sample was sandwiched between a microscope slide and a coverslip for observation under a fluorescence microscope (Leica DM6000) with the LAX capture software.

Details of the synthesis of the thio-N-acetylgalactosamine-PEG-sulfate ligand (S-GalNAc-PEG-sulfate)

^{1}H-NMR and ^{13}C-NMR spectra of the products are reported in the Annex at the end of the ESI.

Synthesis of 3,4,6-triacetoxy galactosyl thiazoline **2**

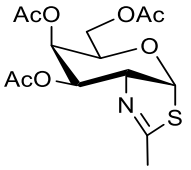

Commercially available 2-acetamido-2-deoxy-1,3,4,6-tetra-oacetyl-β-D-galactopyranose **1** (1.5 g, 3.85 mmol, 1 eq) and Lawesson's reagent (1.87 g, 4.62 mmol, 1.2 eq) were dissolved in 12.5 mL of anhydrous toluene and stirred at 353 K under argon atmosphere. After 24 hours, the resulting suspension was neutralized with 124.7 mg of sodium bicarbonate. Toluene was then evaporated, and the crude product was purified by chromatographic column using a mixture of ethyl acetate and hexane (1:1) as the eluent. 942 mg (71%) of pure product was obtained.

$[\alpha]^{20}_{D}$: 96.9 (c 0.8, $CHCl_3$)

^{1}H RMN (400MHz, $CDCl_3$): δ 6.27 (d, 1H, $J_{1,2}$=6.31Hz, H-1), 5.54 (t, 1H, $J_{3,4}$=$J_{4,5}$=3.32Hz, H-4), 5.23 (dd, 1H, $J_{3,2}$=8.00Hz, $J_{3,4}$=3.40Hz, H-3), 4.41 (t, 1H, $J_{2,1}$=$J_{2,3}$=7.15Hz, H-2), 4.34-4.29 (m, 1H, H-5), 4.28-4.21 (m, 1H, H-6a), 4.15-4.09 (m, 1H, H-6b), 2.29 (d, 3H, J=1.61Hz, C-CH_3), 2.15 (s, 3H, -COO-CH_3), 2.11 (s, 3H, -COO-CH_3), 2.08 (s, 3H, -COO-CH_3). **^{13}C RMN (100MHz, $CDCl_3$):** δ 170.5 (CO), 170.2 (CO), 169.8 (CO), 168.5 (=C-), 89.0 (C1), 74.5 (C2), 70.6 (C5), 70.5(C3), 66.3 (C4), 60.9 (C6), 21.4 (C-CH_3), 20.9 (-COO-CH_3), 20.7 (-COO-CH_3), 20.6 (-COO-CH_3).

HRMS: Calcd. for $C_{14}H_{21}O_7NS$ 346.0955 $[M+H]^+$, found 346.0952.

Synthesis of Thiol **3**

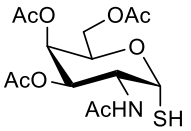

To a mixture of 330 mg (0.85 mmol, 1 eq) of thiazoline **2**, 4.76 mL of MeOH and 0.13 mL of trifluoroacetic acid were added followed by 0.4 mL of water. The mixture was stirred at 273 K for 5 h, the concentrated under vacuum. The crude mixture was purified through column chromatography, using DCM/MeOH (50:1) as the eluent, yielding 260 mg (85%) of pure product.

$[\alpha]^{20}_{D}$: 100 (c 0.7, $CHCl_3$)

^{1}H RMN (400MHz, $CDCl_3$): δ 5.58 (t, 1H, $J_{1,2}$=$J_{1,SH}$=5.80Hz, H-1), 5.73 (d, 1H, $J_{NH,2}$=7.68Hz, NH-COOH-CH_3), 5.41 (d, 1H, $J_{4,3}$=2.40Hz, H-4), 5.09 (dd, 1H, $J_{3,2}$=11.80Hz, $J_{3,4}$=3.20Hz, H-3), 4.81-4.70 (m, 1H, H-2), 4.53 (t, 1H, $J_{5,6a}$=$J_{5,6b}$,48Hz, H-5), 4.22-4.00 (m, 2H, H-6), 2.17 (s, 3H, -COO-CH_3) , 2.06 (s, 3H, -COO-CH_3), 2.03 (s, 3H, -COO-CH_3), 2.00 (s, 3H, -COO-CH_3), 1.96 (d, J=6.6Hz, -SH). **^{13}C RMN (100MHz, $CDCl_3$):** δ 171.1 (CO), 170. 8 (CO), 170.5 (CO), 170.2 (CO), 79.6 (C1), 67.8 (C5), 67.7 (C3), 67.1 (C6), 61.6 (C4), 48.4 (C2), 20.8 (NHCOCH_3), 20.7 (-COO-CH_3), 20.7 (-COO-CH_3), 20.7 (-COO-CH_3).

HRMS: Calcd. for $C_{14}H_{20}O_8NSNa$ 386.0880 $[M+Na]^+$, found 386.0876.

Synthesis of Cyclic Sulfite **5**

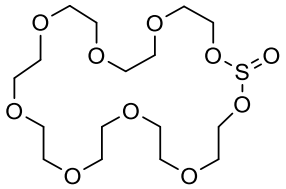

To a solution of commercially available octaethylene glycol (370 mg, 1.35 mmol, 1 eq) and DMAP (8.25 mg, 0.068 mmol, 0.05 eq), 1.14 mL of DIPEA and 48 mL of anhydrous DCM were added under argon atmosphere. The mixture was stirred for 5 minutes at 273K. Finally, 0.2 mL of $SOCl_2$ (325 mg, 2.7 mmol, 2 eq) were gradually added. The mixture was stirred at r.t. for 1 h. Subsequently, it was washed with a saturated NaCl solution and extracted twice with DCM. The resulting solution was dried with $MgSO_4$, filtered, and the DCM evaporated under vacuum. The crude product was purified through column chromatography using DCM:MeOH (30:1) as the eluent, yielding 511 mg (91%) of pure product.

^{1}H RMN (500MHz, $CDCl_3$): δ 4.25-4.10 (m, 4H, 2 -C$\underline{H_2}$-OSO_2-O-), 3.79-3.71 (m, 4H, 2 -CH_2-CH_2-OSO_2-O-), 3.70-3.61 (m, 24H, 12 OCH_2). **^{13}C RMN (125MHz, $CDCl_3$):** δ 70.7 (6 CH_2O-), 70.6 (6 CH_2O-), 69.5 (2 -CH_2-OSO_2-O), 61.5 (2 -CH_2-OSO_2-O).

HRMS: Calcd. for $C_{16}H_{32}O_{10}NaS$ 439.1608 $[M+Na]^+$, found 439.1600

Synthesis of Cyclic Sulfate **6**

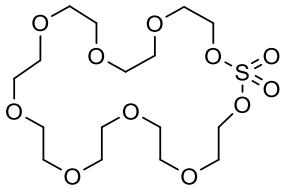

To 1.4 g (3.36 mmol, 1 eq) of cyclic sulfite **5**, 30.7 mL of ACN, 30.7 mL of TCM, and 46 mL of water were added. The mixture was stirred for 5 minutes at 273 K. Then, 1.8 g (8.4 mmol, 2.5 eq) of $NaIO_4$ and 20.91 mg (0.1 mmol, 0.03 eq) of $RuCl_3 \cdot 3H_2O$ were added. The mixture is stirred at room temperature for 4 h. Next, the two obtained phases were separated, and the aqueous phase was washed twice with DCM. The resulting solution of the combined organic phases was dried with $MgSO_4$, filtered, and the solvent was evaporated. The crude product was purified through column chromatography using DCM:MeOH (40:1) as the eluent, yielding 1.15 g (79%) of pure product.

^{1}H RMN (500MHz, $CDCl_3$): δ 4.25 (t, 4H, J=4.61Hz, 2 -C$\underline{H_2}$-OSO_2-O-), 3.62 (t, 4H, J=4.47Hz, 2 -C$\underline{H_2}$-CH_2-OSO_2-O-), 3.52-3.36 (m, 24H, 12 OCH_2). **^{13}C RMN (125MHz, $CDCl_3$):** δ 72.1 (2 -$\underline{C}H_2$-OSO_2-O), 70.5 (9 CH_2O-), 70.4 (3 CH_2O-), 68.1 (2 -$\underline{C}H_2$-OSO_2-O).

HRMS: Calcd. for $C_{16}H_{32}O_{11}NaS$ 455.1557 $[M+Na]^+$, found 455.1548

Synthesis of Sulfate **7**

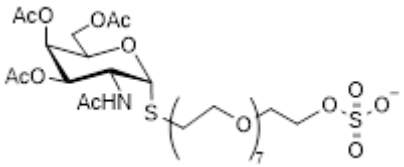

To 50 mg (0.14 mmol, 1 eq) of cyclic sulfate **6**, 0.1 mL of Et_3N (triethylamine) and 0.25 mL of DMF (dimethylformamide) are added. To this solution, another solution containing 116 mg (0.16 mmol, 1.17 eq) of thiol 3 in 0.25 mL of DMF is added. The mixture is stirred at room temperature for 1 hour. The crude product is purified through column chromatography using DCM:MeOH (30:1) as the eluent, yielding 67.6 mg (61%) of pure product.

^{1}H RMN (500MHz, $CDCl_3$): δ 6.23 (d, 1H, $J_{NH,2}$=8.23Hz, NH-COOH-CH_3), 5.62 (d, 1H, $J_{1,2}$=5.24Hz, H-1), 5.42 (s, 1H, H-4), 5.07 (dd, 1H, $J_{3,2}$=11.70Hz, $J_{3,4}$=2.84Hz, H-3), 4.78-4.71 (m, 1H, H-2), 4.56 (t, 1H, $J_{5,6a}$=$J_{5,6b}$=6.40Hz, H-5), 4.23 (t, 2H, J=3.83Hz, CH_2-OSO_3-), 4.17-4.11 (m, 1H, H-6a), 4.11-4.05 (m, 1H, H-6b), 3.77-3.47 (m, 28H, 14 OCH_2), 2.91-2.73 (m, 2H, S-CH_2-CH_2-), 2.16 (s, 3H, -COO-CH_3) , 2.06 (s, 3H, -COO-CH_3), 2.01 (s, 3H, -COO-CH_3), 2.00 (s, 3H, -COO-CH_3). **^{13}C RMN (125MHz, $CDCl_3$):** δ 171.0 (CO), 170.7 (CO), 170.4 (CO), 170.3 (CO), 84.9 (C1), 70.3 (-CH_2-), 70.1 (-CH_2-), 70.0 (-CH_2-), 69.9 (-CH_2-), 69.9 (-CH_2-), 69.7 (-CH_2-), 69.6 (-CH_2-), 69.6 (-CH_2-), 69.6 (-CH_2-), 69.5 (-CH_2-), 69.5 (-CH_2-), 69.4 (-CH_2-), 69.3 (-CH_2-), 68.4 (C3), 67.3 (C4), 67.1 (C5), 66.4 (-CH_2-), 61.2 (C6), 48.3 (C2), 30.2 (-CH_2-), 23.2 (CH_3), 20.8 (CH_3), 20.7 (CH_3), 20.7 (CH_3).

HRMS: Calcd. for $C_{30}H_{53}O_{19}NNaS_2$ 818.2545 $[M+H+Na]^+$, found 818.2542

Synthesis of Ligand **8** (S-GalNAc-PEG-sulfate)

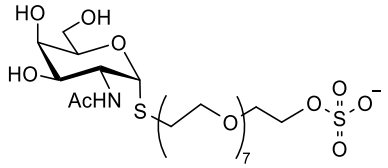

To 60 mg (0.076 mmol, 1 eq) of sulfate 6, 3 mL of MeOH (methanol) and 0.20 mL of MeONa (sodium methoxide) are added. The mixture is stirred at room temperature for 30 minutes under an argon atmosphere. Then, Amberlite is added until the pH of the solution is neutralized. The mixture is filtered, and MeOH is evaporated. 51 mg (100%) of pure product is obtained.

^{1}H RMN (500MHz, MeOD): δ 5.63 (d, 1H, $J_{1,2}$=5.39Hz, H-1), 4.45-4.39 (m, 1H, H-2), 4.22-4.13 (m, 3H, H-5, SO_4-CH_2-), 3.93 (d, 1H, $J_{4,3}$=3.29Hz, H-4), 3.80-3.63 (m, 31H, H-6, H-3, 14 OCH_2), 2.92-2.68 (m, 2H, S-CH_2-CH_2-), 2.00 (s, 3H, -COO-CH_3). **^{13}C RMN (125MHz, MeOD):** δ 172.5 (CO), 84.3 (C1), 71.6 (-CH_2-OSO_3^-), 70.4 (-CH_2-), 69.7 (-CH_2-), 69.7 (-CH_2-), 69.6 (-CH_2-), 69.6 (-CH_2-), 69.6 (-CH_2-), 69.5 (-CH_2-), 69.5 (-CH_2-), 69.5 (-CH_2-), 69.5 (-CH_2-), 69.4 (-CH_2-), 69.4 (-CH_2-), 69.4 (-CH_2-), 69.3 (-CH_2-), 68.9 (C4), 67.9 (C3), 66.8 (C5), 61.4 (C6), 50.5 (C2), 29.2 (-S-CH_2-), 21.3 (CH_3).

MS (ESI, m/z): Calcd for $C_{24}H_{46}O_{16}NS_2^-$ 668.23 $[M]^-$, found 668.39

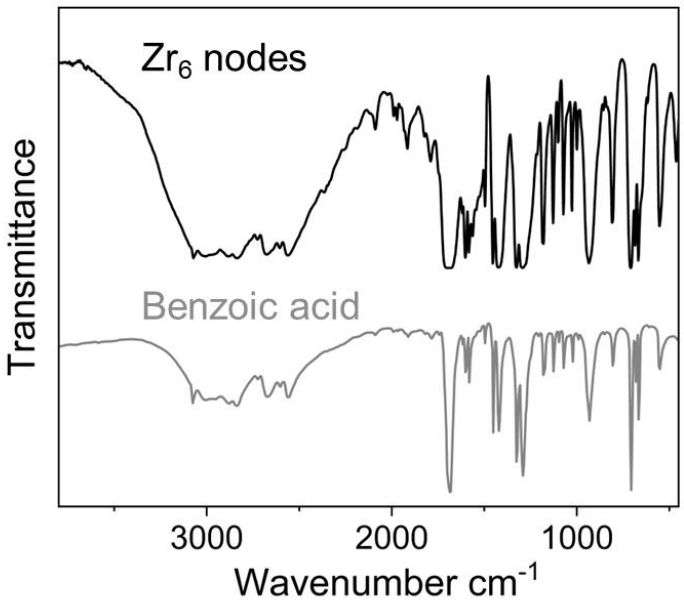

Fig. S3 FTIR analysis of the Zr_6 nodes and of benzoic acid.

S3. Preliminary tests for batch optimization

Table S1 Preliminary optimization for batch synthesis.

Entry	Changed parameter	Space-Time-Yield (STY) (Kg m^{-3} day^{-1})
1	0.5 L:M	3.38±1.1
2	3.5 L:M	11.48±2.8
3	10 mL DMF	2.74±0.8
4	6 mL DMF	5.11±1.2
5	90 µL TFA (L:Mod 0.024)	3.11±0.9
6	150 µL TFA (L:Mod 0.015)	2.97±0.4

Reaction conditions: 393 K, 5 h, 8 mL DMF, 10 mL volume of reactor. Entries 3-6: 22.5 mg TCPP (0.0284 mmol, 3.55 mM), 38 mg Zr_6 nodes (L:M 0.9). Entries 1-4:130 µL TFA (L:Mod 0.017).

Table S2 Experimental details for the optimization of the ligand-to-metal center molar ratio (L:M) in batch.

Entry	Mass Zr_6 nodes (mg)	Mol Zr_6 nodes	L:M	STY (Kg m^{-3} day^{-1})	TCPP conversion (%)	Size (nm)
1	13	0.0112	2.5	3.4±0.3	22.1±1.9	101±9
2	16	0.0137	2	3.5±0.5	22.7±3.2	114±10
3	25	0.0215	1.3	3.8±0.4	24.7±2.6	132±11
4	33	0.0284	1	5.5±0.6	35.7±3.8	222±12
5	45	0.0387	0.7	6.0±0.5	38.9±3.2	248±19
6	70	0.0601	0.5	7.1±0.7	46.1±4.5	250±25
7	90	0.0773	0.4	10.1±0.4	65.6±2.6	273±80
8	120	0.1031	0.3	11.5±0.8	74.7±5.2	287±110

Reaction conditions: 393 K, 5 h, 22.5 mg TCPP (0.0284 mmol, 3.55 mM), 8 mL DMF, 130 µL TFA (L:Mod 0.017), 10 mL volume of reactor. Theoretical yield 32.25 mg of PCN-222 (theoretical STY: 15.36 Kg m^{-3} day^{-1}).

Table S3 Green metrics of selected experiments for the optimization of the ligand-to-metal center molar ratio (L:M) in batch.

Entry	L:M	Mass of reagents (mg)	Mass waste (mg)	PCN-222 (mg)	E-factor no solvents	RME(%) no solvents	E-factor with solvents
4	1	249.2	237.7	11.5	20.7	4.6	1129
5	0.7	261.2	248.7	12.5	19.9	4.8	1040
6	0.5	286.2	271.4	14.8	18.3	5.2	879

Reaction conditions: 393 K, 5 h, 22.5 mg TCPP (0.0284 mmol), 8 mL DMF, 130 µL TFA (L:Mod 0.017), 10 mL volume of reactor. When solvents were considered for E-factor calculations, a total of 11 mL of DMF (8 mL for reaction, 3 mL for washing) and 3 mL of EtOH were used. Densities for DMF and EtOH are 0.944 and 0.789 g mL^{-1} respectively.

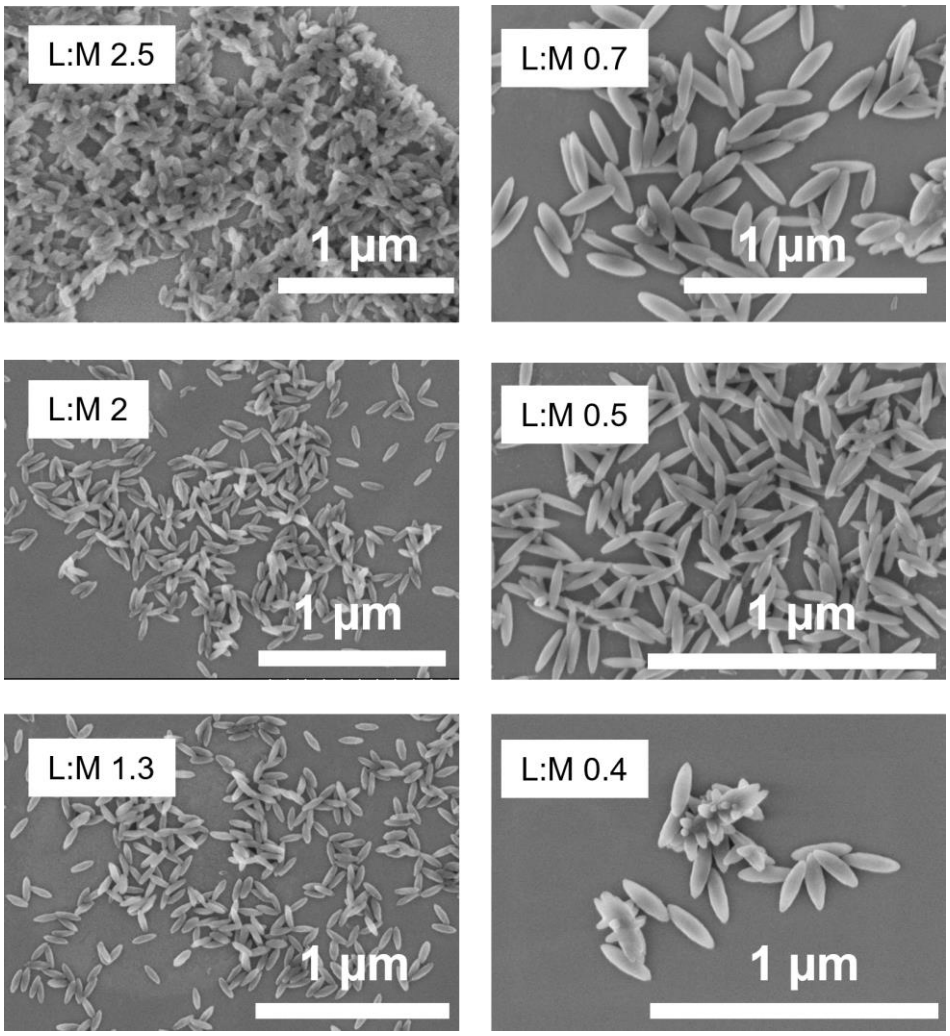

Fig. S4 SEM images of the experiments for the optimization of the ligand-to-metal center molar ratio (L:M) in batch.

S4. Relevant publications related to the c.f. synthesis of MOFs

Table S4 Most relevant publications reporting the c.f. synthesis of different MOFs.

Type of MOF	T (K)	Pressure	Residence time	Rate or Space Time Yield (STY)	Size (nm)	Ref.
UiO-66	393	100	3 sec	104 g h^{-1}	211	1
MOF-808	423	/	5 min	95155 kg m^{-3} day^{-1}	140	2
UMCM-1, MUF-77	358	5	/	1.15 g h^{-1}	100	3
UiO-66-NH_2, Zr-fumarate	363	/	5.5 h	7.3 g h^{-1}	>2000	4
UiO-66, Fe–BTC, MIL-100	388	/	63 sec	19.6 kg m^{-3} day^{-1}	>1000	5
MOF-801, MOF-804, MOF-808, DUT-67	273	/	32-80 min	367.2 kg m^{-3} day^{-1}	100-500	6
Ni_2Cl_2(BTDD)	413	/	30-60 min	1 kg $month^{-1}$	1000	7
ZIF-8	273	/	30 sec	5 mL min^{-1}	40-100	8
MOF-74(Ni)	343	/	/	90 g h^{-1} l^{-1}	>1000	9
HKUST-1	343	/	/	6.32 ·10^5 kg m^{-3} day^{-1}	>1000	10
UiO-66	363	/	22 min	0.24 mL min^{-1}	>1000	11
$MgFe_2O_4$@UiO-66-NH_2	403	10	15min	215.3 kg m^{-3} day^{-1}	20-200	12
UiO-67	413	/	30 min	428 kg m^{-3} day^{-1}	200-400	13
MIL-53(Al)	523	/	/	1300 kg m^{-3} day^{-1}	/	14
MIL-53(Cr)	423	5	3.5 min	7188 kg m^{-3} day^{-1}	200-1000	15
UiO-66-$(OH)_2$, Zr-fumarate, Zr-mesaconate, DUT-67, MOF-808	358	/	22 min	2733 kg m^{-3} day^{-1}	/	16
UiO-66(Zr)-$(OH)_2$	383	/	10 min	6.79 g h^{-1}	10-200	17
UiO-67	393	/	10 min	6.10 g h^{-1}	/	18
HKUST-1	343	10	70-167 sec	2685 kg m^{-3} day^{-1}	100-250	19
CPO-27-Ni	363	/	20 min	2 mL min^{-1}	40	20
ZrBTB	403	/	32 min	385.03 kg m^{-3} day^{-1}	>1000	21
MIL-100	383	/	50 min	771.6 kg m^{-3} day^{-1}	100-500	22
MIL-88 serie	368	/	20-600 sec	103-618 µl min^{-1}	90-900	23
Ln-BTC·$6H_2O$	333	/	50 min	426 kg m^{-3} day^{-1}	200-300	24
ZIF-67	393	/	3 min	57000 kg m^{-3} day^{-1}	150-400	25

/=not reported

S5. Calculation of Re, De and residence time (τ)

Table S5 Parameters of Reactor 1.

REACTOR 1	
Lenght	560 cm
Diameter	0.08 cm
Volume	2.8 mL
Hellicoid heightº	6 cm
Radius of the curvature	2.85 cm
DMF density	0.944 g mL^{-1}
DMF Dinamic Viscosity	0.0089 g cm^{-1} s^{-1}

Table S6 Data of the flow pattern of Reactor 1.

Flow (mL min^{-1})	**Fluid velocity (cm s^{-1})**	**Re**	**De**	**τ (sec)**
0.1	0.33	2.8	0.3	1680
0.2	0.67	5.7	0.7	840
0.3	1.00	8.5	1.0	560
0.5	1.67	14.1	1.7	336
1	3.33	28.3	3.4	168
2	6.67	56.6	6.7	84
3	10.00	84.9	10.1	56
4	13.33	113.1	13.4	42
5	16.67	141.4	16.8	33.6
10	33.33	282.8	33.5	16.8

S6. Details of the effect of the concentration of the reagents, the volumetric flow rate, the amount of employed acid modulator, and the temperature of the reactions on the STY and on the size-distribution of PCN-222

Concentration of the reagents (volume of solvent)

Table S7 Experimental details for the optimization of the concentration of the reagents in c.f.

Entry	[TCPP] (mM)	STY (Kg m^{-3} day^{-1})	Size (nm)
1	7.1	486±24	232±60
2	5.7	324±18	166±32
3	4.7	238±22	131±20
4	4.1	151±10	125±19
5	3.6	108±12	99±15
6	3.2	53±8	91±19

Reaction conditions: 393 K, total flow 1 mL min^{-1}, L:M=1, L:Mod=0.027, solvent DMF, 2.8 mL volume of the reactor.

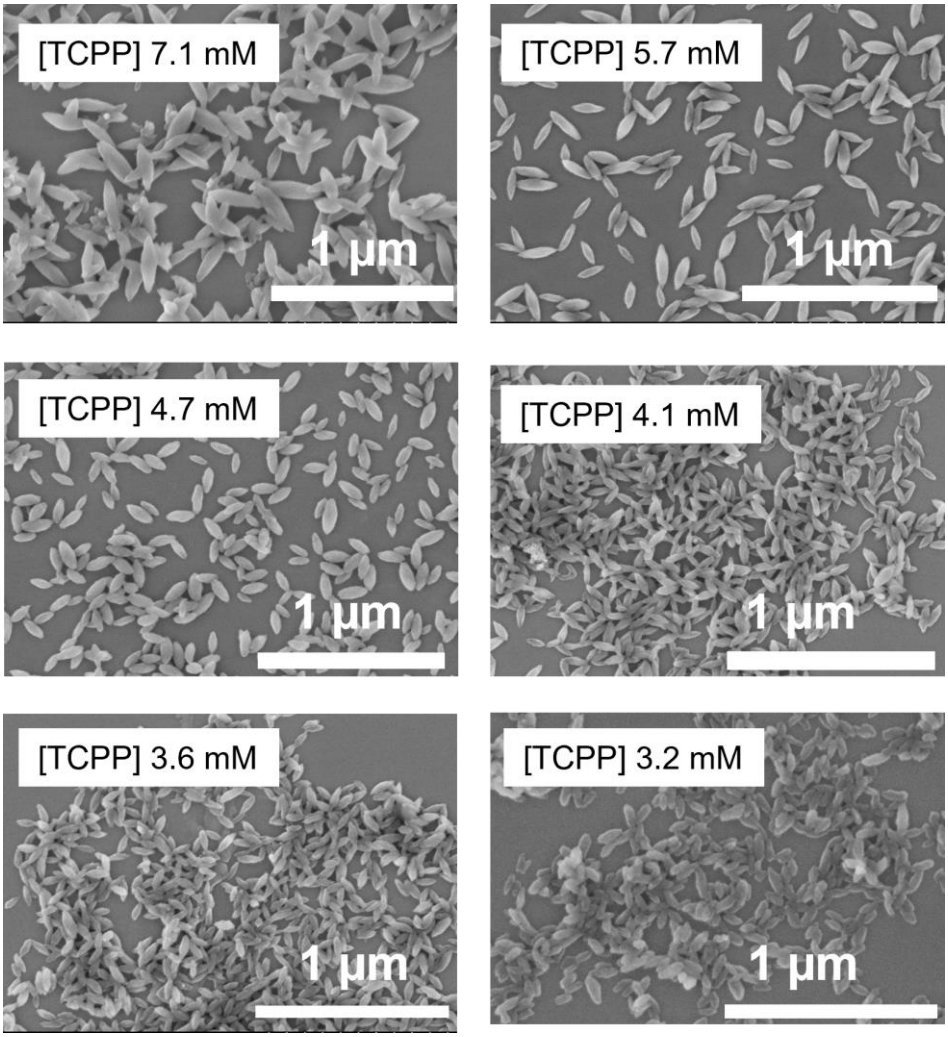

Fig. S5 SEM images of the experiments for the optimization of the concentration of the reagents in c.f..

Table S8 Green metrics of the experiments of the optimization of the concentration of the reagents in c.f..

Entry	[TCPP] (mM)	E-factor no solvents	RME(%)no solvents	E-factor with solvents
1	7.1	45.4	2.2	1,377
2	5.7	54.9	1.8	2,053
3	4.7	61.7	1.6	2,782
4	4.1	85.3	1.2	4,374
5	3.6	104.9	0.9	6,101
6	3.2	190.8	0.5	12,409

Reaction conditions: 393 K, total flow 1 mL min^{-1}, L:M=1, L:Mod=0.027, solvent DMF, 2.8 mL volume of the reactor. When solvents were considered for E-factor calculations, a total of 3.15 mL of DMF (for reaction and for washing) and 0.7 mL of EtOH were used for the volume of the reactor. Densities for DMF and EtOH are 0.944 and 0.789 g mL^{-1} respectively.

Flow rate

Table S9 Experimental details for the optimization of the flow rate..

Entry	Flow rate (mL min^{-1})	STY (Kg m^{-3} day^{-1})	TCPP Conv (%)	Size (nm)
1	0.1	40±9	14.7±3.3	90±50
2	0.2	84±6	15.4±1.1	98±42
3	0.3	118±15	14.4±1.8	113±40
4	0.5	161±12	11.8±0.9	118±14
5	1	252±15	9.2±0.5	125±16
6	2	517±25	9.5±0.5	97±18
7	3	734±31	8.9±0.4	96±16
8	4	749±33	6.9±0.3	95±20
9	5	744±24	5.5±0.2	87±19

Reaction conditions: 393 K, [TCPP]=4.7 mM. L:M=1, L:Mod=0.027, solvent DMF, 2.8 mL volume of the reactor.

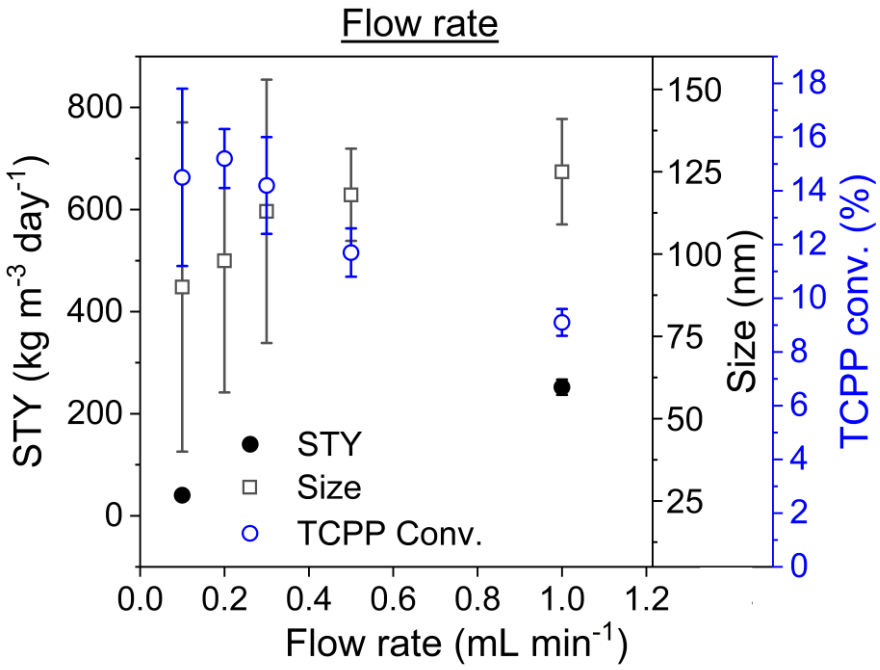

Fig. S6 Details of the effect of the flow rate (0.1-1 mL min^{-1}) on the STY and on the size-distribution of PCN-222.

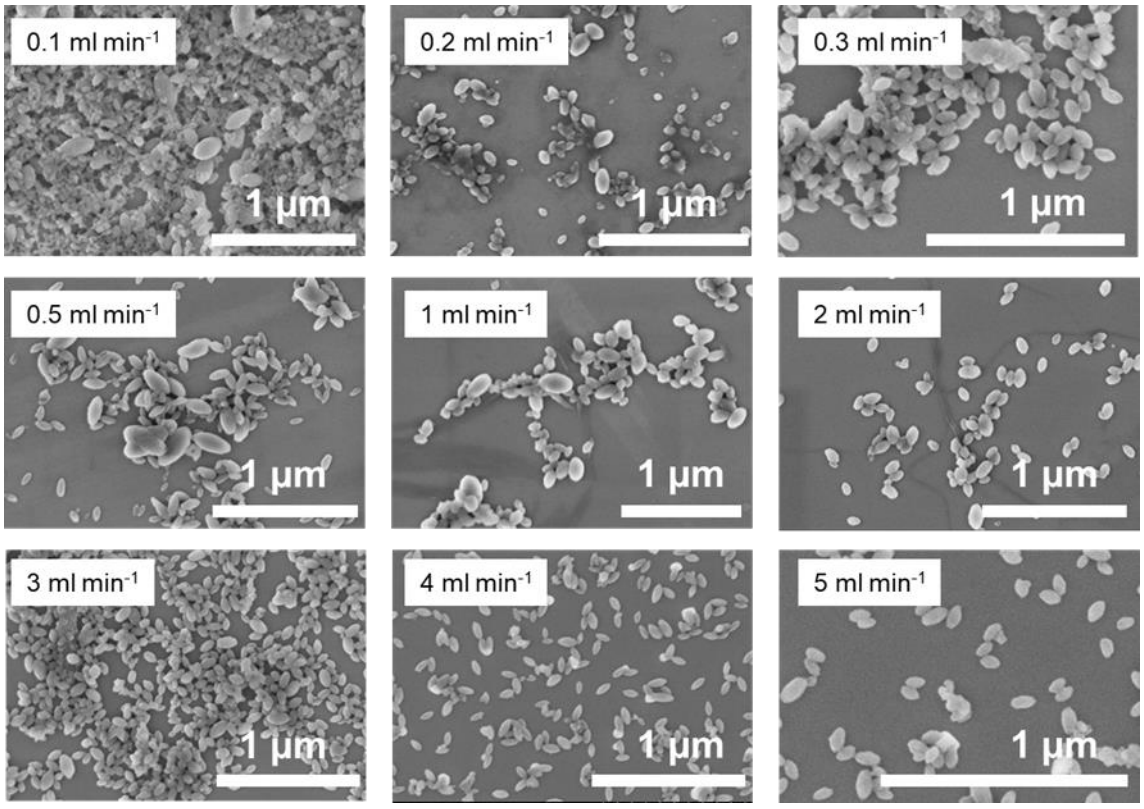

Fig. S7 SEM images of the experiments for the optimization of the flow rate.

Table S10 Green metrics of the experiments of the optimization of the flow rate.

Entry	Flow rate (mL min^{-1})	E-factor no solvents	RME(%)no solvents	E-factor with solvents
1	0.1	37.6	2.6	1,657
2	0.2	35.8	2.7	1,578
3	0.3	38.2	2.5	1,685
4	0.5	46.9	2.1	2,058
5	1	60.3	1.6	2,630
6	2	58.7	1.7	2,564
7	3	62.1	1.6	2,709
8	4	81.4	1.2	3,540
9	5	102.7	1.0	4,455

Reaction conditions: 393 K, [TCPP]=4.7 mM. L:M=1, L:Mod=0.027, solvent DMF, 2.8 mL volume of the reactor. When solvents were considered for E-factor calculations, a total of 3.15 mL of DMF (for reaction and for washing) and 0.7 mL of EtOH were used for the volume of the reactor. Densities for DMF and EtOH are 0.944 and 0.789 g mL^{-1} respectively.

Acid modulator

Table S11 Experimental details for the optimization of the acid modulator concentration in c.f..

Entry	L:Mod	STY (Kg m^{-3} day^{-1})	Size (nm)
1	0.054	385±28	n.d.
2	0.036	809±41	44±35
3	0.027	801±65	93±28
4	0.022	694±54	98±12
5	0.018	667±33	105±18
6	0.015	478±20	153±25
7	0.011	231±28	210±35
8	0.007	184±23	n.d.

Reaction conditions: 393 K, L:M=1, flow rate 3 mL min^{-1}, [TCPP]=4.7 mM, flow rate 3 mL min^{-1}, solvent DMF, 2.8 mL volume of the reactor.

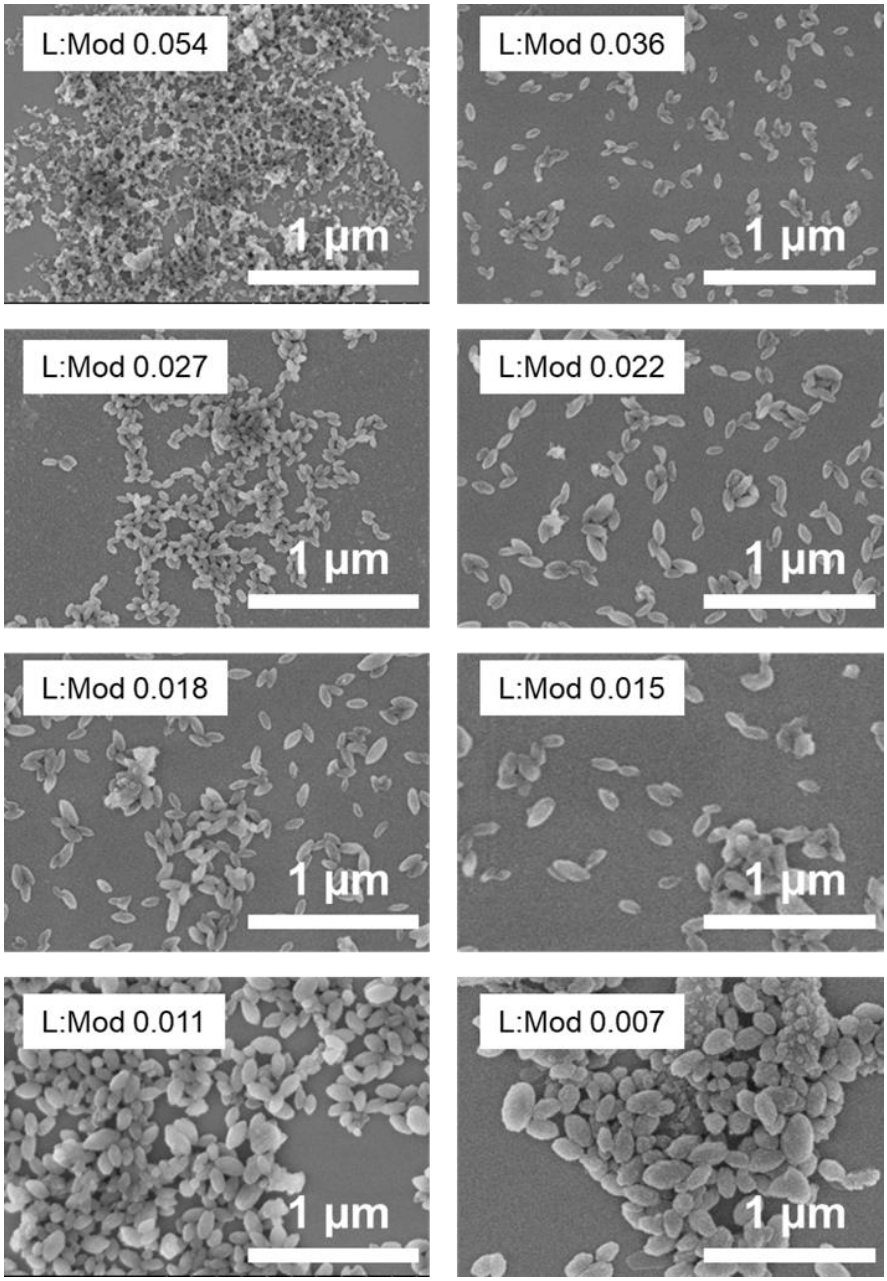

Fig. S8 SEM images of the experiments for the optimization of the acid modulator concentration in c.f..

Table S12 Green metrics of the experiments of the optimization of the acid modulator concentration in c.f..

Entry	L:Mod	E-factor no solvents	RME(%)no solvents	E-factor with solvents
1	0.054	79.5	1.2	5,126
2	0.036	46.8	2.1	2,448
3	0.027	56.8	1.7	2,482
4	0.022	75.8	1.3	2,875
5	0.018	91.4	1.1	3,004
6	0.015	147.1	0.7	4,212
	0.011	392.3	0.3	8,803
	0.007	726.1	0.1	11,285

Reaction conditions: 393 K, L:M=1, flow rate 3 mL min^{-1}, [TCPP]=4.7 mM, flow rate 3 mL min^{-1}, solvent DMF, 2.8 mL volume of the reactor. When solvents were considered for E-factor calculations, a total of 3.15 mL of DMF (for reaction and for washing) and 0.7 mL of EtOH were used for the volume of the reactor. Densities for DMF and EtOH are 0.944 and 0.789 g mL^{-1} respectively.

Temperature

Table S13 Experimental details for the optimization of the temperature of the reaction in c.f..

Entry	Temperature (K)	STY (Kg m^{-3} day^{-1})	SEM size (nm)
1	383	386±32	77±12
2	388	568±37	83±12
3	393	738±51	108±13
4	398	864±44	109±15
5	403	926±58	111±16
6	408	972±36	115±16
7	413	1002±47	113±27
8	418	n.d.	n.d.

Reaction conditions: L:M=1, L:Mod=0.027, [TCPP]=4.7 mM, flow rate 3 mL min^{-1}, solvent DMF, 2.8 mL volume of the reactor.

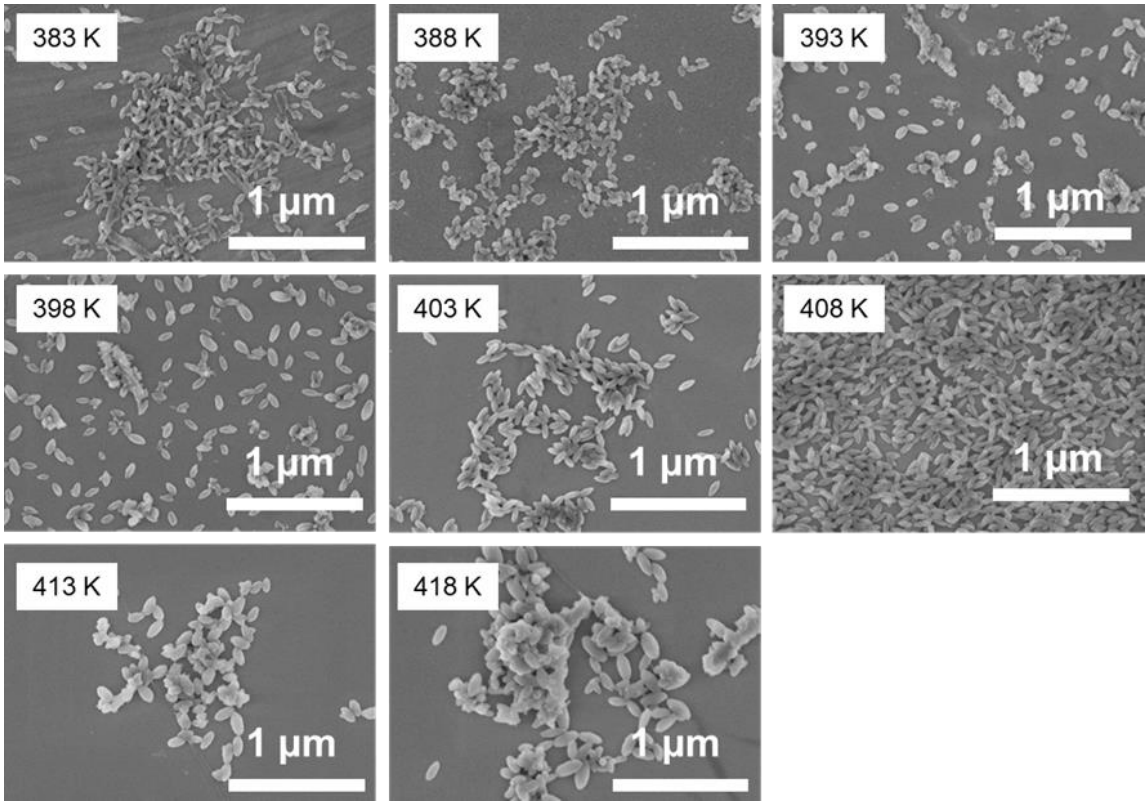

Fig. S9 SEM images of the experiments for the optimization of the temperature of the reaction in c.f..

Table S14 Green metrics of the experiments for the optimization of the temperature of the reaction in c.f..

Entry	Temperature (K)	E-factor no solvents	RME(%)no solvents	E-factor with solvents
1	383	119.0	0.8	5,152
2	388	80.5	1.2	3,501
3	393	61.7	1.6	2,694
4	398	52.6	1.9	2,301
5	403	49.0	2.0	2,147
6	408	46.6	2.1	2,045
7	413	45.2	2.2	1,984
8	418	n.d.	n.d.	n.d.

Reaction conditions: L:M=1, L:Mod=0.027, [TCPP]=4.7 mM, flow rate 3 mL min^{-1}, solvent DMF, 2.8 mL volume of the reactor. When solvents were considered for E-factor calculations, a total of 3.15 mL of DMF (for reaction and for washing) and 0.7 mL of EtOH were used for the volume of the reactor. Densities for DMF and EtOH are 0.944 and 0.789 g mL^{-1} respectively.

S7. Residence time distribution and pulse experiment

In a pulse input experiment, an amount of pulse tracer is rapidly injected in one shot into the feed stream entering the reactor. Thus, the outlet concentration is measured as a function of time. TCPP was selected as tracer since it's one of the reagents and considering its UV-Vis absorption spectrum. Initially, a calibration curve was determined varying the concentration of TCPP from 0.05 to 0.00025 mM, as shown in Fig. S10.

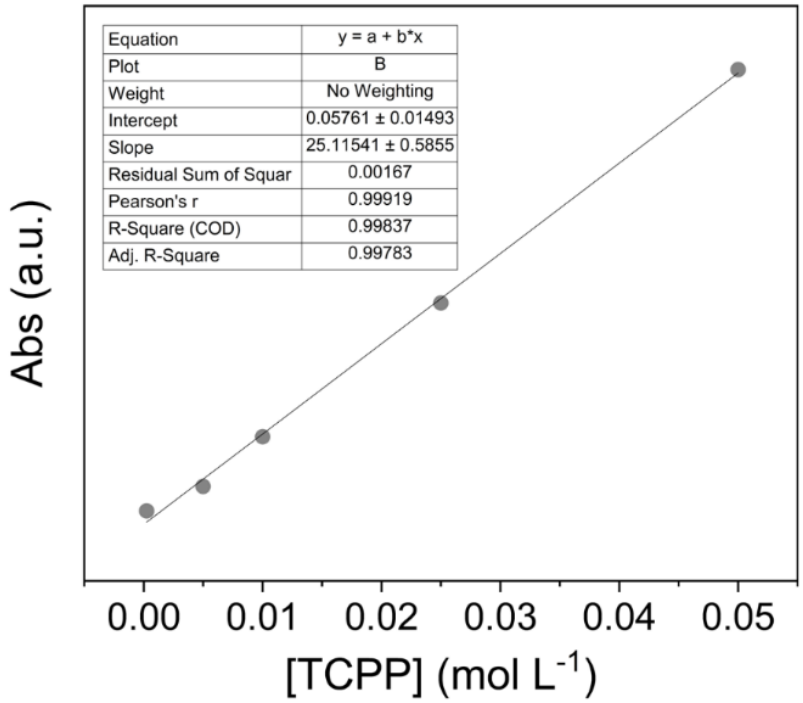

Fig. S10 Calibration curve for the pulse input experiment using TCPP as pulse tracer.

Thus, the experiment was performed obtaining the curve of the concentration in function of time C(t), which was thus converted into E(t) by dividing the curve C(t) with the integral of the same curve, as shown in Fig. S11 (a) and (b).

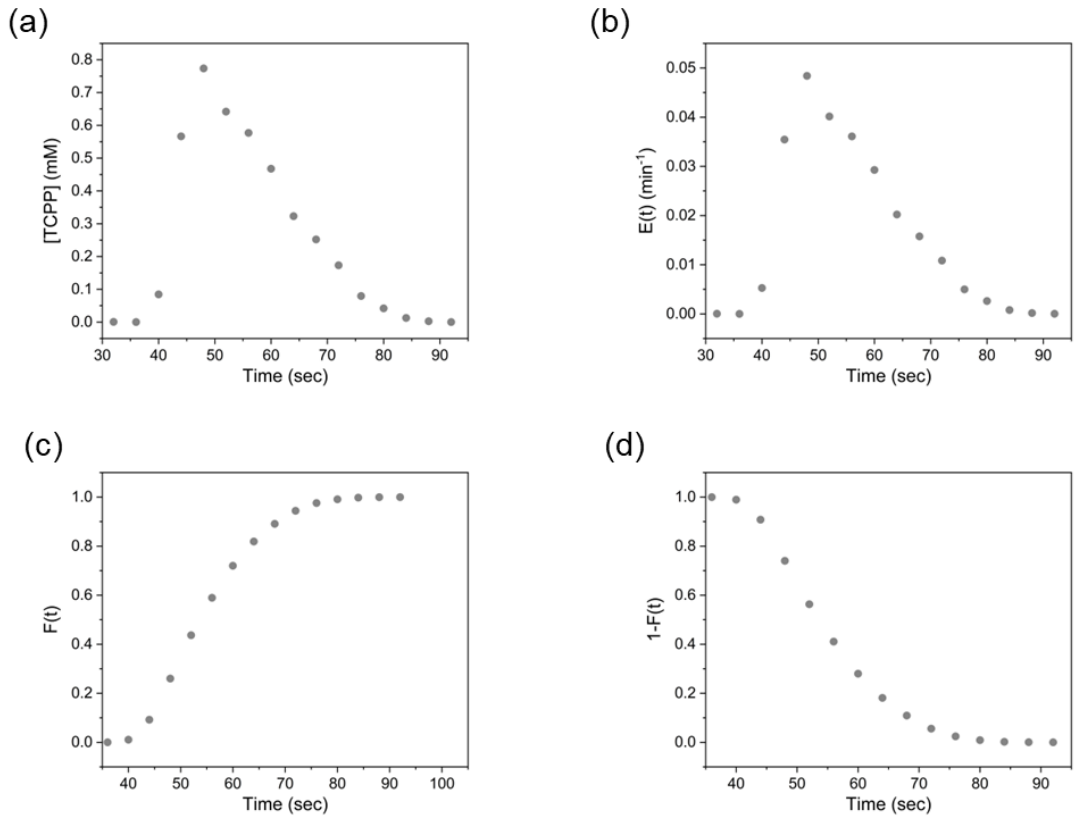

Fig. S11 (a) C(t), (b) E(t), (c) F(t) and (d) 1-F(t) curves of the pulse input experiment.

It was observed that ca. 60% of the solution passed through the reactor within the theoretical τ (56 seconds), as also highlighted by the cumulative distribution function F(t) and by 1-F(t) shown in Fig. S11 (c) and (d). Table S15 reports the data used for the calculations.

Table S15 Experimental data of the pulse input experiment.

time (sec)	[TCPP] (mM)	E (t)	F(t)	1-F(t)
32	6.58E-04	4.11E-05	0	1
36	2.00E-04	1.25E-05	1.07E-04	0.99989
40	0.08436	0.00528	0.01068	0.98932
44	0.56662	0.03544	0.09211	0.90789
48	0.7737	0.04839	0.25977	0.74023
52	0.64191	0.04015	0.43684	0.56316
56	0.57688	0.03608	0.5893	0.4107
60	0.46774	0.02925	0.71997	0.28003
64	0.3231	0.02021	0.81889	0.18111
68	0.25215	0.01577	0.89085	0.10915
72	0.17322	0.01083	0.94406	0.05594
76	0.07958	0.00498	0.97568	0.02432
80	0.04186	0.00262	0.99087	0.00913
84	0.01269	7.93E-04	0.99769	0.00231
88	0.00275	1.72E-04	0.99962	3.80E-04
92	2.85E-04	1.78E-05	1	2.05E-07

S8. US-assisted techniques

Table S16 Experimental details for the optimization of the US-etching in c.f..

Entry	US amplitude (%)	STY (Kg m^{-3} day^{-1})	Size (nm)	Aspect ratio
1	0	980±55	122±8	2.11±0.19
2	30	894±78	124±18	2.47±0.25
3	60	786±45	129±14	2.58±0.29
4	90	756±68	125±21	2.90±0.26

Reaction conditions: 408 K, L:M=1, L:Mod=0.036, [TCPP]=4.7 mM, flow rate 3 mL min^{-1}, solvent DMF, 2.8 mL + 2.8 mL volume of the reactor(s).

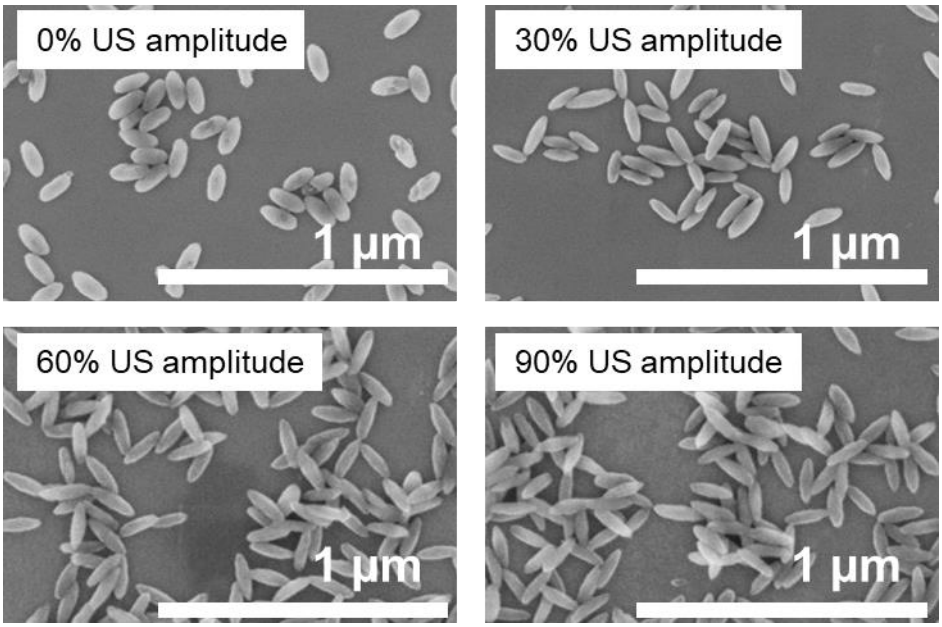

Fig. S12 SEM images of the experiments for the optimization of the US-etching in c.f. Reaction conditions: 408 K, L:M=1, L:Mod=0.036, [TCPP]=4.7 mM, flow rate 3 mL min^{-1}, solvent DMF.

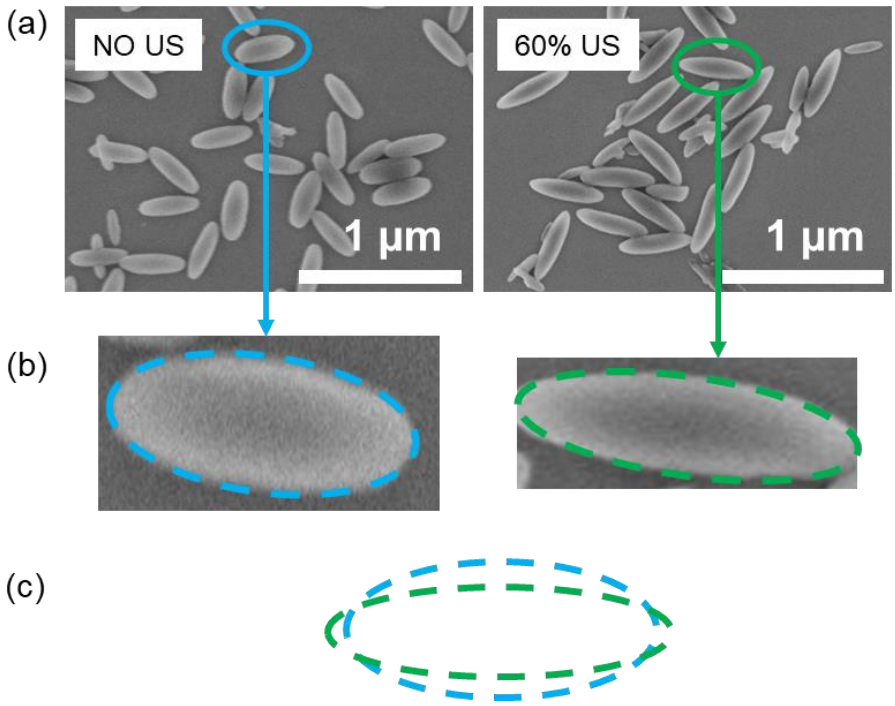

Fig. S13 (a) SEM images, (b) details and (c) overlapping of the dimension of two selected particles for the study of the effect of US-etching in c.f. using larger PCN-222 particles. Reaction conditions: 408 K, L:M=1, L:Mod=0.036, [TCPP]=4.7 mM, flow rate 3 mL min^{-1}, solvent DMF.

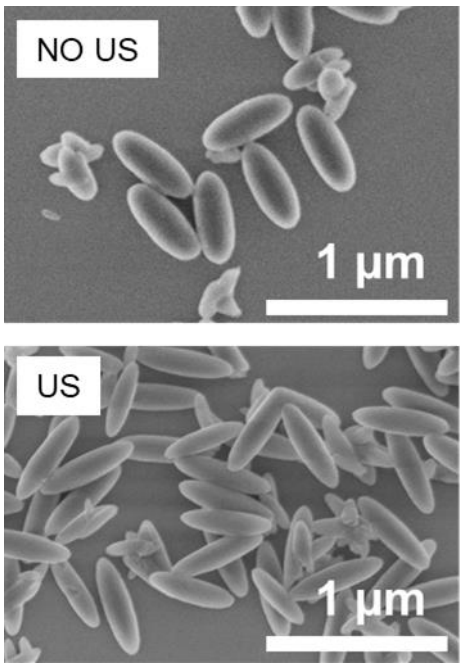

Fig. S14 SEM images of the experiments for the study of the effect of US-etching in batch (using an US bath for 30 minutes). Reaction conditions for the synthesis of PCN-222: 393 K, 5 h, 22.5 mg TCPP (0.0284 mmol), 38 mg Zr_6 nodes (L:M=0.9), 8 mL DMF, 350 µL TFA (L:Mod= 0.006).

S9. DLS analysis of the samples PCN-222(0%US) and PCN-222(60%US)

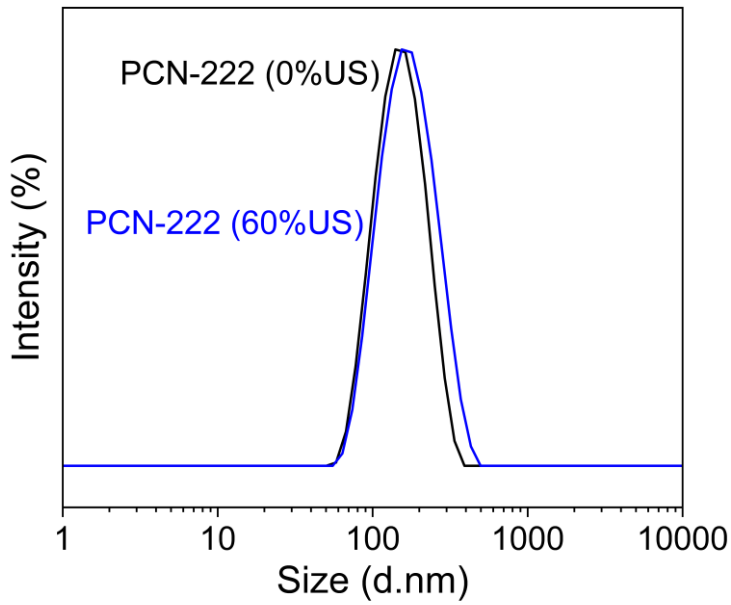

Fig. S15 DLS curves of the samples PCN-222(0%US) and PCN-222(60%US). Hydrodynamic dimensions were 154±36 nm and 178±42 nm respectively. Reaction conditions: 408 K, L:M=1, L:Mod=0.036, [TCPP]=4.7 mM, flow rate 3 mL min^{-1}, solvent DMF, 2.8 mL + 2.8 mL volume of the reactor.

S10. Green approach of the c.f. synthesis

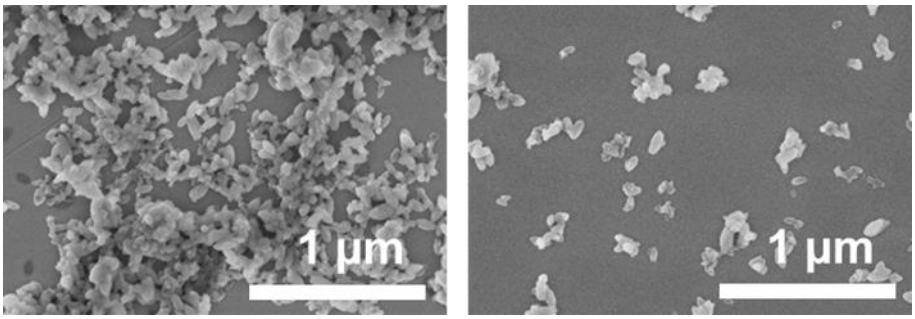

Fig. S16 SEM images of the synthesis in c.f. using a mixture 1:1 cyclohexane:DMF as solvent. Reaction conditions: 408 K, L:M=1, L:Mod=0.036, [TCPP]=4.7 mM, flow rate 3 mL min^{-1}.

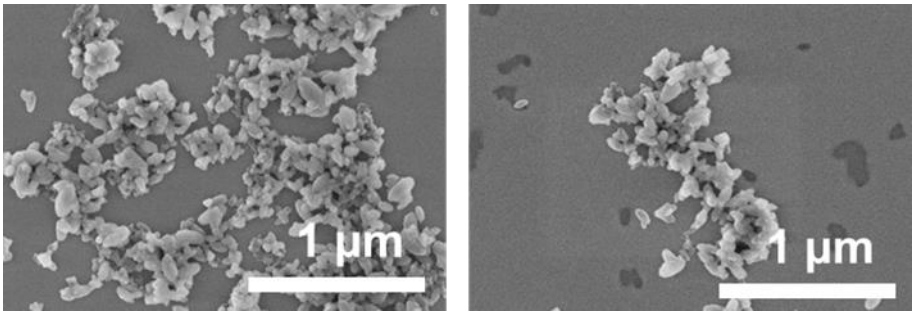

Fig. S17 SEM images of the synthesis in c.f. using a mixture 1:1 anisole:DMF as solvent. Reaction conditions: 408 K, L:M=1, L:Mod=0.036, [TCPP]=4.7 mM, flow rate 3 mL min^{-1}.

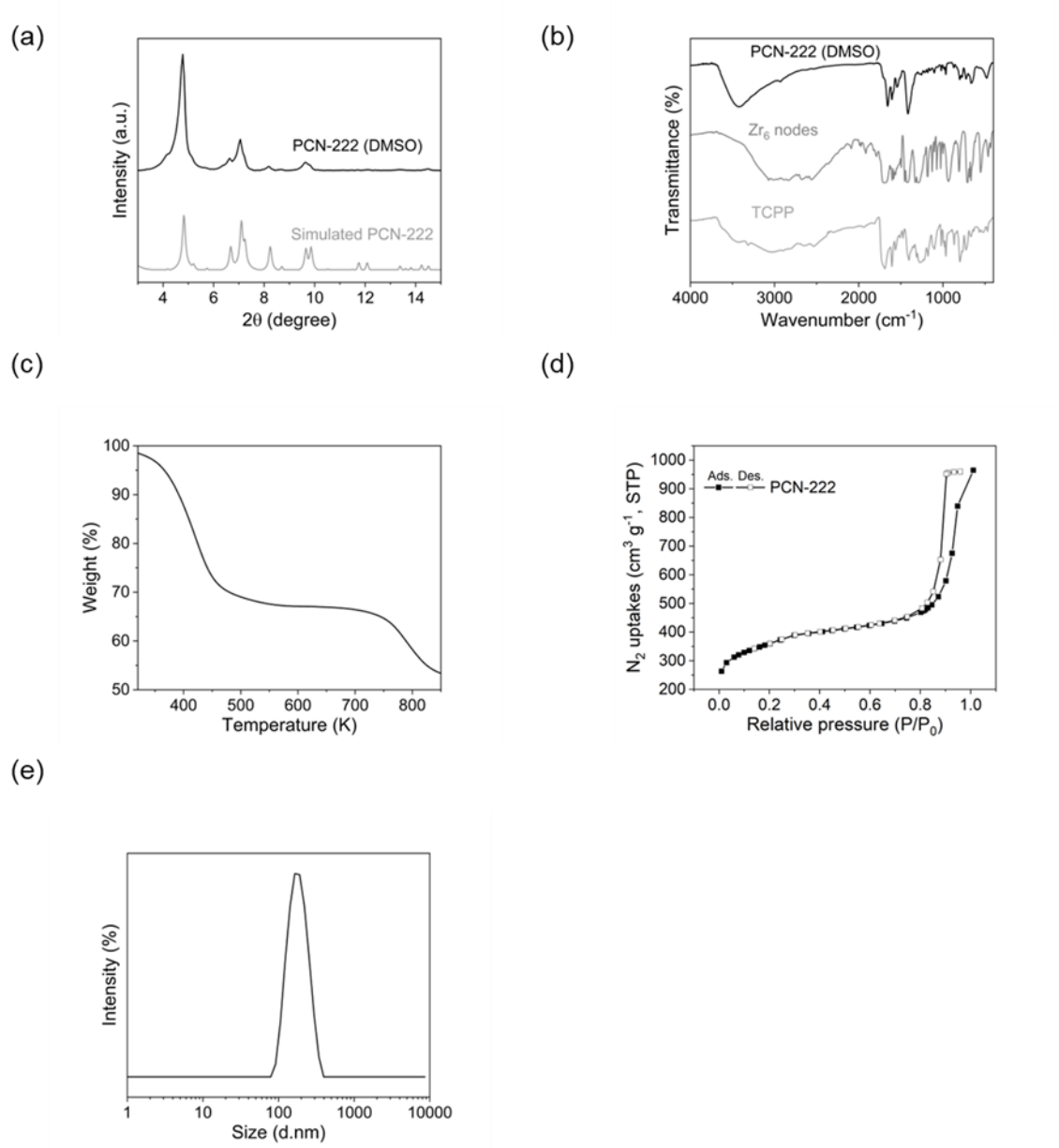

Fig. S18 (a) PXRD patterns, (b) FTIR analysis, (c) details of TGA analysis (d) N_2 absorption/desorption isotherm and (e) DLS curve of PCN-222 produced using DMSO as solvent. Reaction conditions: 408 K, L:M=1, L:Mod=0.036, [TCPP]=4.7 mM, flow rate 3 mL min^{-1}.

Table S17 Experimental details for the optimization of the temperature using DMSO as solvent in c.f.

Entry	Temperature (K)	STY (Kg m^{-3} day^{-1})	Size (nm)
1	403	956±18	238±76
2	413	1003±34	485±111
3	433	1065±66	521±103
4	423	1173±74	536±185

Reaction conditions: L:M=1, L:Mod=0.036, [TCPP]=4.7 mM, flow rate 3 mL min^{-1}, solvent DMSO.

Table S18 Green metrics of the experiments of the optimization of the temperature of the reaction

Entry	Temperature (K)	E-factor no solvents	RME(%)no solvents	E-factor with solvents
1	403	39.4	2.5	2,355
2	413	37.5	2.6	2,245
3	433	35.3	2.8	2,114
4	423	32.0	3.0	1,919

Reaction conditions: L:M=1, L:Mod=0.036, [TCPP]=4.7 mM, flow rate 3 mL min^{-1}, solvent DMSO. When solvents were considered for E-factor calculations, a total of 3.15 mL of DMSO (for reaction and for washing) and 0.7 mL of EtOH were used for the volume of the reactor. Densities for DMSO and EtOH are 1.100 and 0.789 g mL^{-1} respectively.

Table S19 Experimental details for the optimization of acid modulator concentration using DMSO as solvent in c.f..

Entry	L:Mod	STY (Kg m^{-3} day^{-1})	Size (nm)
1	0.054	1173±25	116±26
2	0.044	1110±18	331±95
3	0.036	941±35	503±121
4	0.015	679±14	1053±318

Reaction conditions: 423 K, L:M=1, [TCPP]=4.7 mM, flow rate 3 mL min^{-1}, solvent DMSO.

Table S20 Green metrics of the experiments for the optimization of acid modulator concentration using DMSO as solvent in c.f..

Entry	L:Mod	E-factor no solvents	RME(%)no solvents	E-factor with solvents
1	0.054	25.4	3.8	1,913
2	0.044	30.1	3.2	2,024
3	0.036	40.1	2.4	2,392
4	0.015	103.3	1.0	3,363

Reaction conditions: 423 K, L:M=1, [TCPP]=4.7 mM, flow rate 3 mL min^{-1}, solvent DMSO. When solvents were considered for E-factor calculations, a total of 3.15 mL of DMSO (for reaction and for washing) and 0.7 mL of EtOH were used for the volume of the reactor. Densities for DMSO and EtOH are 1.100 and 0.789 g mL^{-1} respectively.

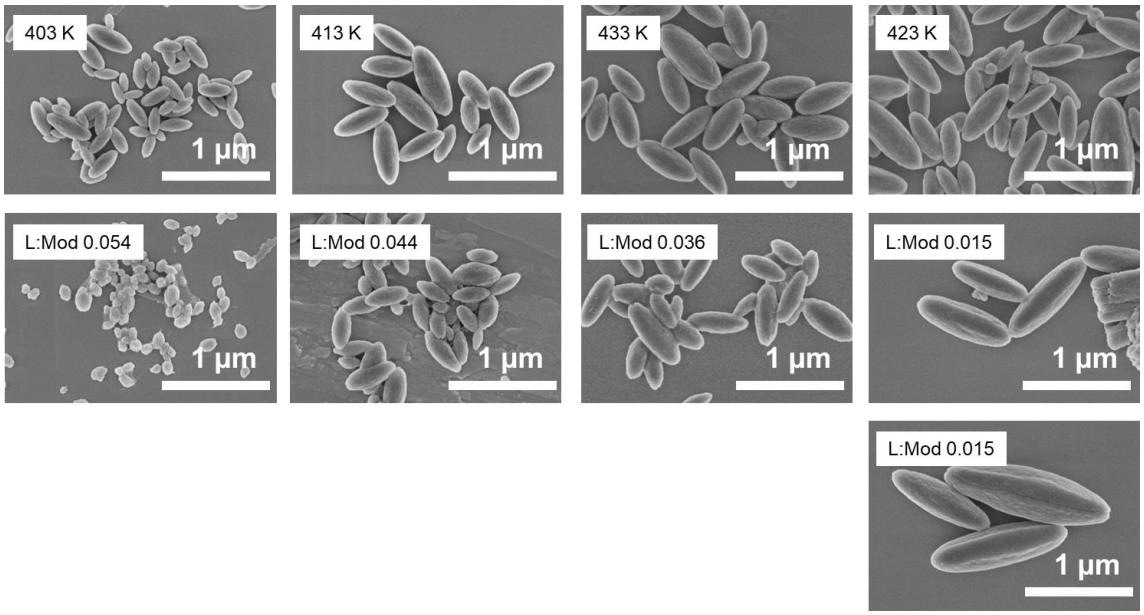

Fig. S19 SEM images for the optimization of acid modulator concentration using DMSO as solvent in c.f..

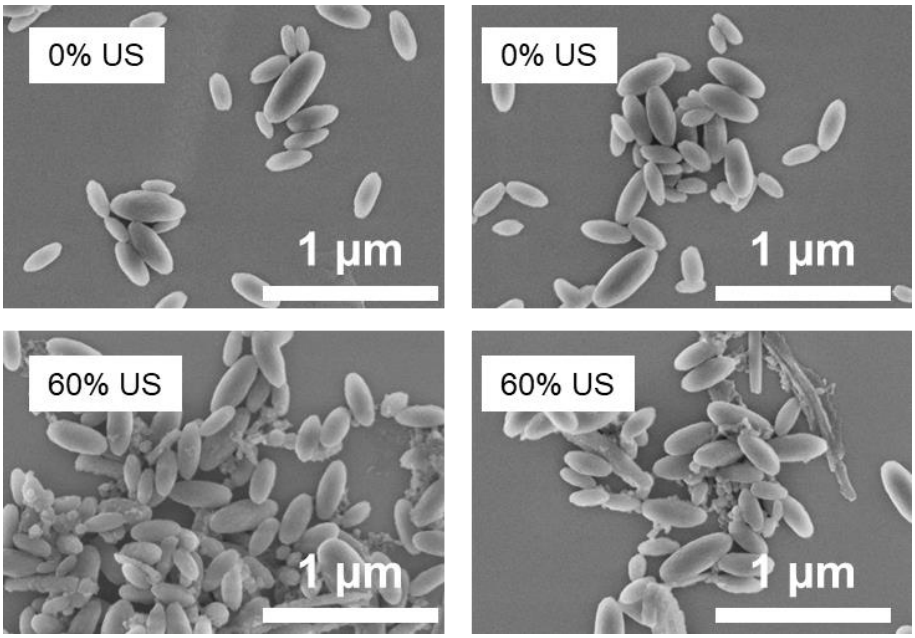

Fig. S20 SEM images for the optimization of the US-etching in c.f. using DMSO as solvent. Reaction conditions: 408 K, L:M=1, L:Mod=0.036, [TCPP]=4.7 mM, flow rate 3 mL min^{-1}.

S11. Functionalization with S-GalNAc-PEG-sulfate ligand

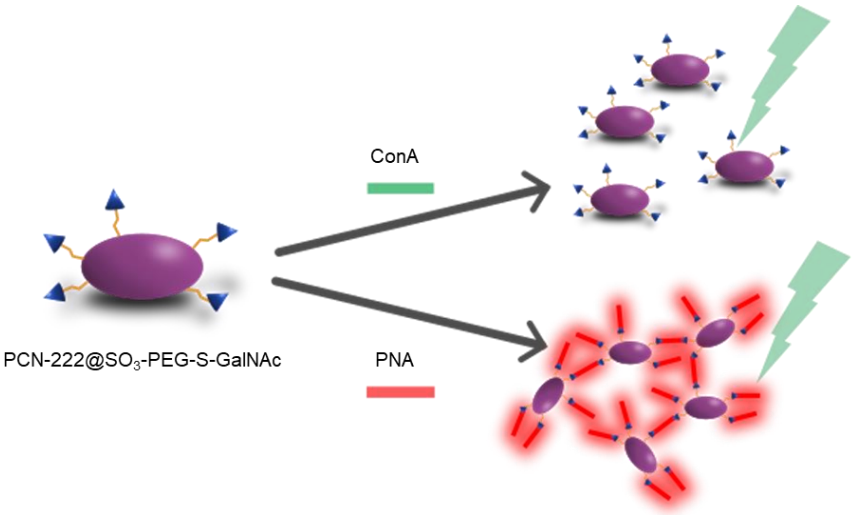

Fig. S21 Scheme of the fluorescence microscopy experiment of selective interaction of the PCN@SO_3-PEG-S-GalNAc with lectins.

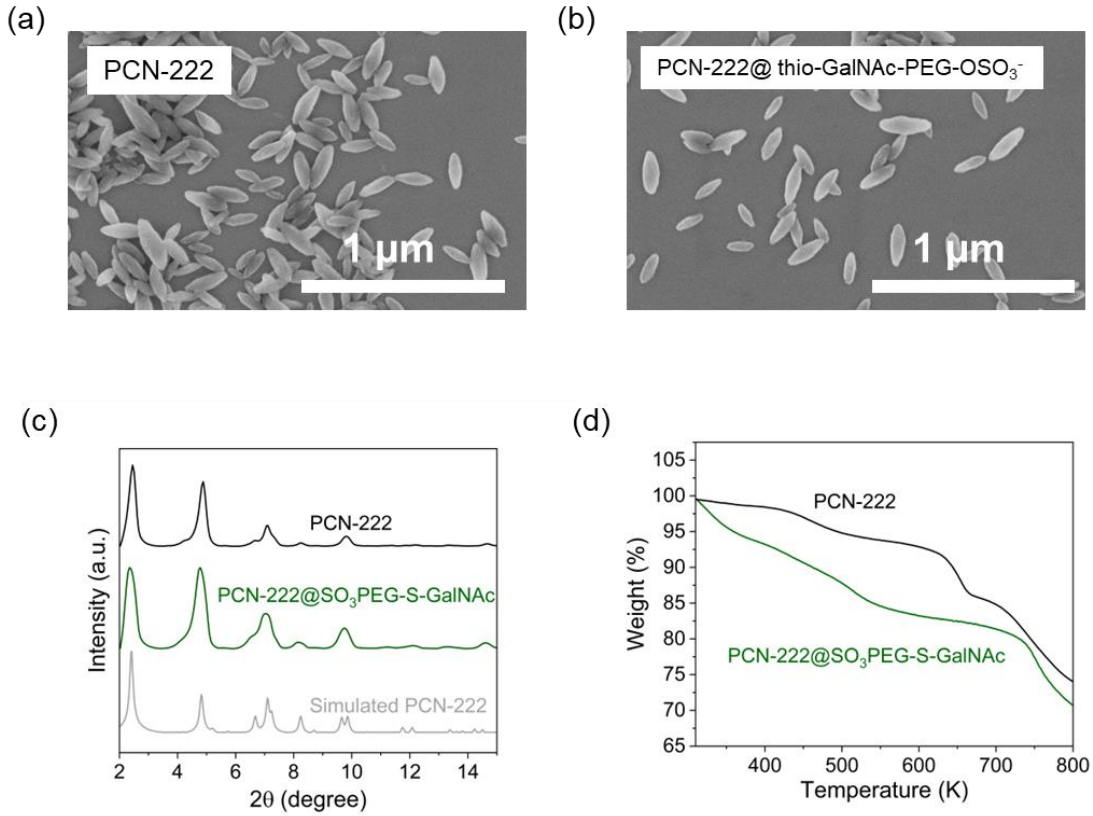

Fig. S22 (a), (b) SEM images; (C) XRD patterns and (d) TGA curves of PCN-222 and PCN-222@ligand in c.f. Reaction conditions: 408 K, L:M=1, L:Mod=0.036, [TCPP]=4.7 mM, flow rate of the MOF 3 mL min^{-1}, flow rate of the mixture of the ligand (in concentration 5 mg mL^{-1}) 3 mL min^{-1}, solvent DMF.

S12. References

1 E. G. Rasmussen, J. Kramlich and I. V. Novosselov, *ACS Sustain Chem Eng*, 2020, **8**, 9680–9689.
2 S. Bagi, S. Yuan, S. Rojas-Buzo, Y. Shao-Horn and Y. Román-Leshkov, *Green Chem*, 2021, **23**, 9982–9991.
3 B. He, L. K. Macreadie, J. Gardiner, S. G. Telfer and M. R. Hill, *ACS Appl Mater Inter*, 2021, **13**, 54284–54293.
4 C. Avci-Camur, J. Troyano, J. Pérez-Carvajal, A. Legrand, D. Farrusseng, I. Imaz and D. Maspoch, *Green Chem*, 2018, **20**, 873–878.
5 L. Garzón-Tovar, M. Cano-Sarabia, A. Carné-Sánchez, C. Carbonell, I. Imaz and D. Maspoch, *React Chem Eng*, 2016, **1**, 533-539.
6 Y. Wang, L. Li, L. Yan, L. Cao, P. Dai, X. Gu and X. Zhao, *Chinese Chem Lett*, 2018, **6**, 849-853.
7 S. Bagi, A. M. Wright, J. Oppenheim, M. Dincă and Y. Román-Leshkov, *ACS Sustain Chem Eng*, 2021, **9**, 3996-4003.
8 F. Carraro, J. D. Williams, M. Linares-Moreau, C. Parise, W. Liang, H. Amenitsch, C. Doonan, C. O. Kappe and P. Falcaro, *Angew Chem Int Ed*, 2020, **59**, 8123-8127.
9 G. H. Albuquerque, R. C. Fitzmorris, M. Ahmadi, N. Wannenmacher, P. K. Thallapally, B. P. McGrail and G. S. Herman, *CrystEngComm*, 2015, **17**, 5502-5510.
10 A. Laybourn, A. M. López-Fernández, I. Thomas-Hillman, J. Katrib, W. Lewis, C. Dodds, A. P. Harvey and S. W. Kingman, *Chem Eng J*, 2019, **359**, 170-177.
11 A. Polyzoidis, M. Schwarzer, S. Loebbecke and C. G. Piscopo, *Mater Lett*, 2017, **197**, 213-216.
12 B. He, M. M. Sadiq, M. P. Batten, K. Suzuki, M. Rubio-Martinez, J. Gardiner and M. R. Hill, *Chem-Eur J*, 2019, **25**, 13184-13188.
13 T. Bailey, M. Pinto, N. Hondow and K. J. Wu, *MethodsX*, 2021, **8**, 101246.
14 P. A. Bayliss, I. A. Ibarra, E. Pérez, S. Yang, C. C. Tang, M. Poliakoff and M. Schröder, *Green Chem*, 2014, **16**, 3796-3802.
15 F. Xue, J. Cao, X. Li, J. Feng, M. Tao and B. Xue, *J Mater Chem C*, 2021, **9**, 7568-7574.
16 H. Reinsch, S. Waitschat, S. M. Chavan, K. P. Lillerud and N. Stock, *Eur J Inorg Chem*, 2016, **27**, 4490-4498.
17 T. K. Vo, V. C. Nguyen, D. T. Quang, B. J. Park and J. Kim, *Micropor Mesopor Mater*, 2021, **312**, 110746.
18 T. K. Vo, V. N. Le, D. T. Quang, M. Song, D. Kim and J. Kim, *Micropor Mesopor Mater*, 2020, **306**, 110405.
19 E. G. Rasmussen, J. Kramlich and I. V. Novosselov, *Chem Eng J*, 2022, **450**, 138053.
20 T. Didriksen, A. I. Spjelkavik and R. Blom, *J Flow Chem*, 2017, **7**, 13-17.
21 Y. Wang, L. Li, L. Yan, X. Gu, P. Dai, D. Liu, J. G. Bell, G. Zhao, X. Zhao and K. M. Thomas, *Chem Mater*, 2018, **30**, 3048-3059.
22 V. N. Le, H. T. Kwon, T. K. Vo, J. H. Kim, W. S. Kim and J. Kim, *Mater Chem Phys*, 2020, **253**, 123278.
23 L. Paseta, B. Seoane, D. Julve, V. Sebastián, C. Téllez and J. Coronas, *ACS Appl Mater Interfaces*, 2013, **5**, 9405-9410.
24 W. Yu, H. Chen, H. Wu, P. Lin, H. Xu, Q. Xie, K. Shi, G. Xie and Y. Chen, *J Alloys Compd*, **890**, 161860.
25 M. Zhang, Z. Yu, Z. Sun, A. Wang, J. Zhang, Y. Y. Liu and Y. Wang, *Micropor Mesopor Mater*, 2021, **327**, 111423.

S13. Annex: ^{1}H-NMR and ^{13}C-NMR spectra

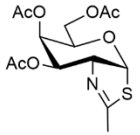

2

^{1}H NMR (400MHz, $CDCl_3$): δ 6.27 (d, 1H, $J_{1,2}$=6.31Hz, H-1), 5.54 (t, 1H, $J_{3,4}$=$J_{4,5}$=3.32Hz, H-4), 5.23 (dd, 1H, $J_{3,2}$=8.00Hz, $J_{3,4}$=3.40Hz, H-3), 4.41 (t, 1H, $J_{2,1}$=$J_{2,3}$=7.15Hz, H-2), 4.34-4.29 (m, 1H, H-5), 4.28-4.21 (m, 1H, H-6a), 4.15-4.09 (m, 1H, H-6b), 2.29 (d, 3H, J=1.61Hz, C-CH_3), 2.15 (s, 3H, -COO-C$\underline{H}_3$), 2.11 (s, 3H, -COO-C$\underline{H}_3$), 2.08 (s, 3H, -COO-C$\underline{H}_3$).

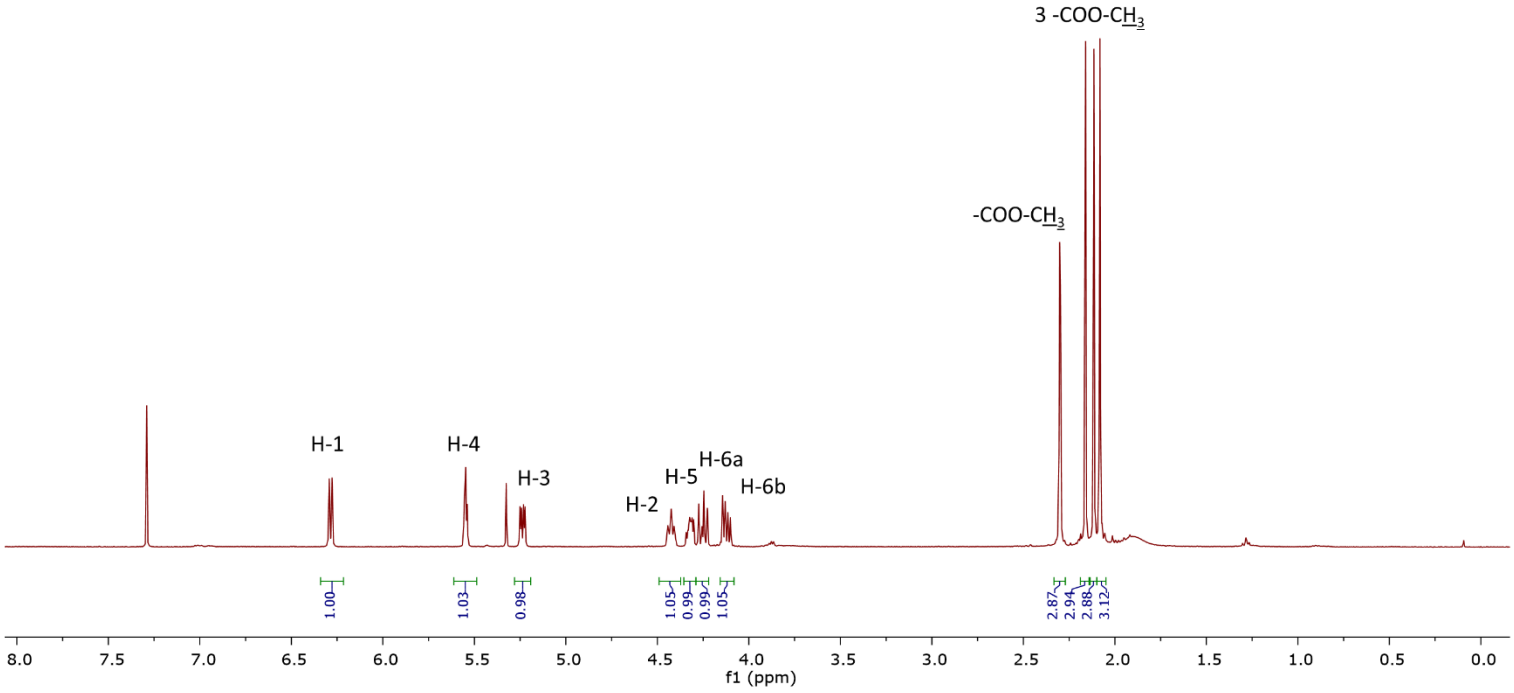

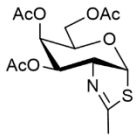

2

^{13}C NMR (100MHz, $CDCl_3$): δ 170.5 (CO), 170.2 (CO), 169.8 (CO), 168,5 (=C-), 89.0 (C1), 74.5 (C2), 70.6 (C5), 70.5(C3), 66.3 (C4), 60.9 (C6), 21.4 (C-$\underline{C}H_3$), 20.9 (-COO-$\underline{C}H_3$), 20.7 (-COO-$\underline{C}H_3$), 20.6 (-COO-$\underline{C}H_3$).

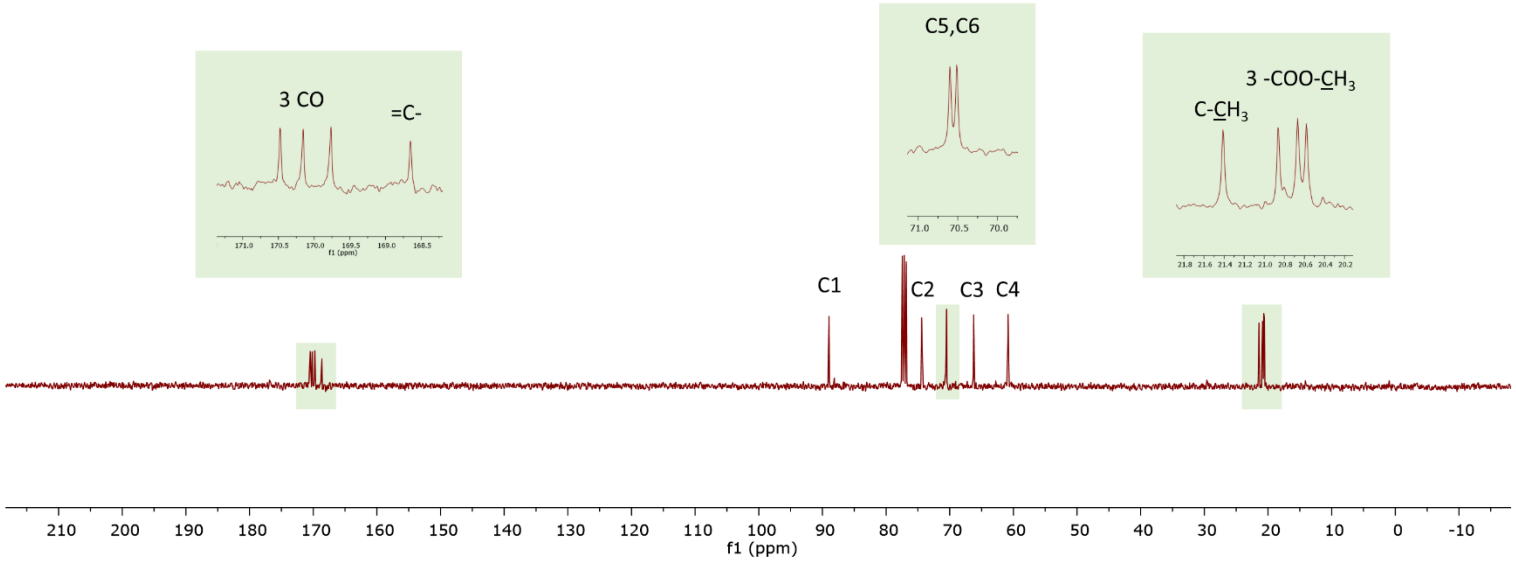

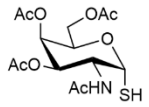

3

^{1}H NMR (400MHz, $CDCl_3$): δ 5.58 (t, 1H, $J_{1,2}$=$J_{1,SH}$=5.80Hz, H-1), 5.73 (d, 1H, $J_{NH,2}$=7.68Hz, NH-COOH-CH_3), 5.41 (d, 1H, $J_{4,3}$=2.40Hz, H-4), 5.09 (dd, 1H, $J_{3,2}$=11.80Hz, $J_{3,4}$=3.20Hz, H-3), 4.81-4.70 (m, 1H, H-2), 4.53 (t, 1H, $J_{5,6a}$=$J_{5,6b}$,48Hz, H-5), 4.22-4.00 (m, 2H, H-6), 2.17 (s, 3H, -COO-CH_3) , 2.06 (s, 3H, -COO-CH_3), 2.03 (s, 3H, -COO-CH_3), 2.00 (s, 3H, -COO-CH_3), 1.96 (d, J=6.6Hz, -SH).

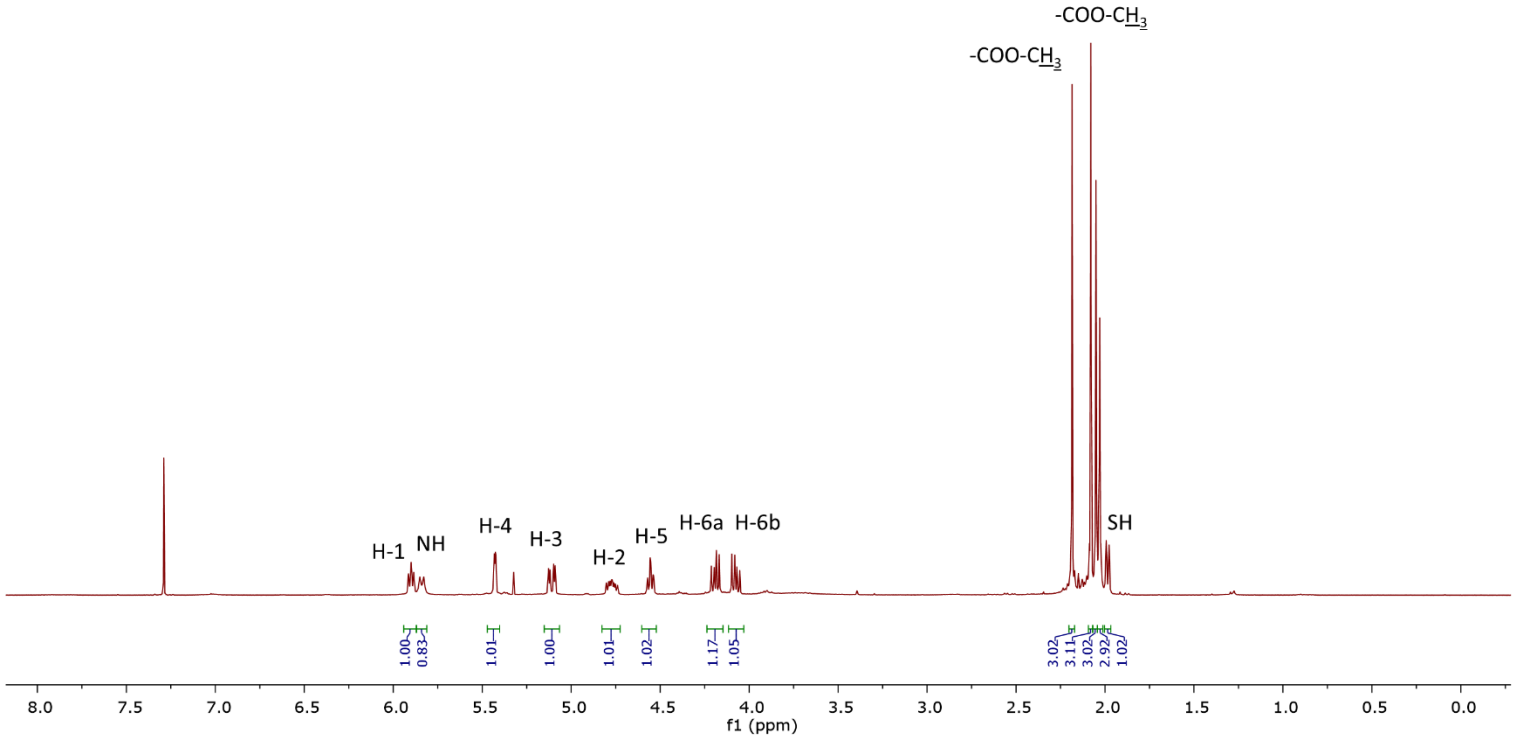

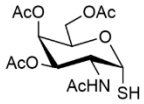

3

^{13}C NMR (100MHz, $CDCl_3$): δ 171.1 (CO), 170.8 (CO), 170.5 (CO), 170.2 (CO), 79.6 (C1), 67.8 (C5), 67.7 (C3), 67.1 (C6), 61.6 (C4), 48.4 (C2), 20.8 ($NHCO\underline{C}H_3$), 20.7 (-COO-$\underline{C}H_3$), 20.7 (-COO-$\underline{C}H_3$), 20.7 (-COO-$\underline{C}H_3$).

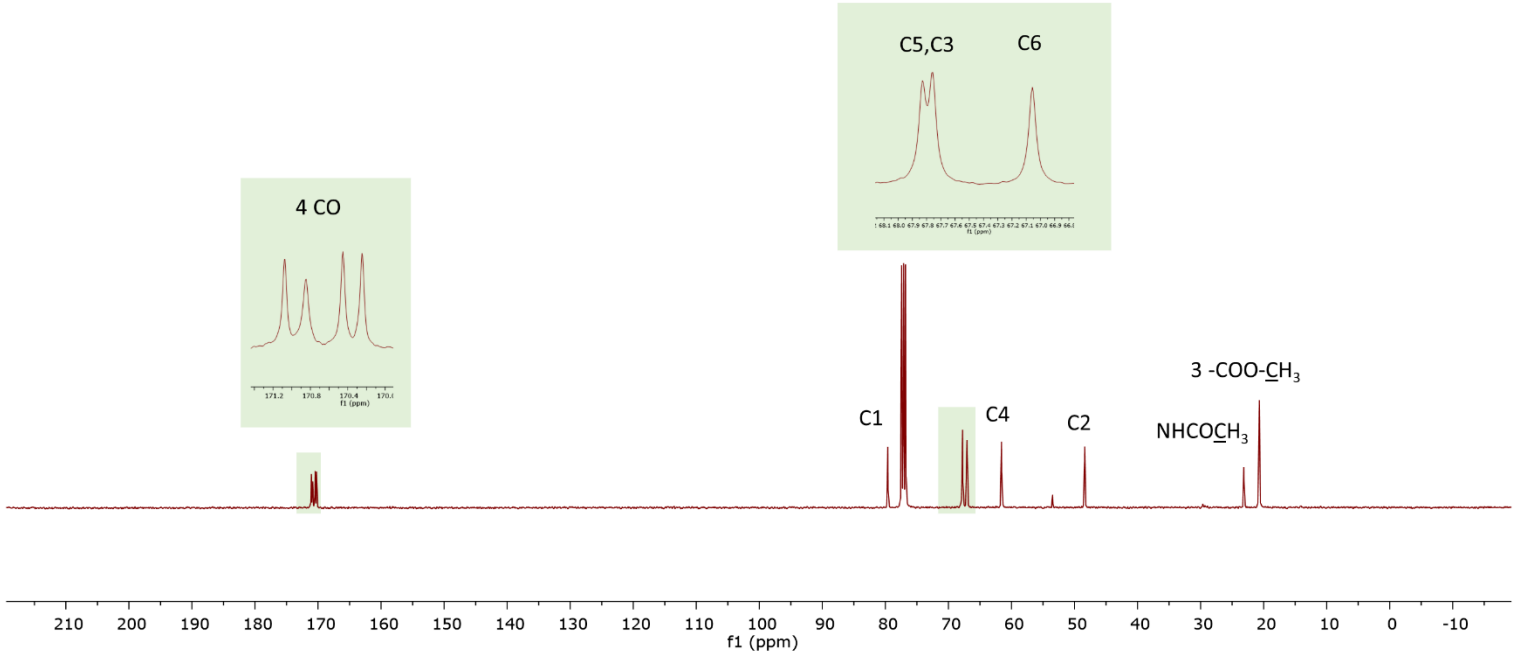

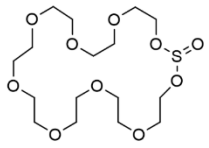

5

^{1}H NMR (500MHz, $CDCl_3$): δ 4.25-4.10 (m, 4H, 2 -C<u>H$_2$</u>-OSO$_2$-O-), 3.79-3.71 (m, 4H, 2 -C<u>H$_2$</u>-CH$_2$-OSO$_2$-O-), 3.70-3.61 (m, 24H, 12 OCH_2).

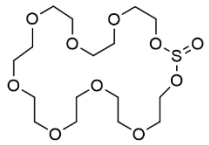

5

^{13}C NMR (125MHz, $CDCl_3$): δ 70.7 (6 -CH_2O-), 70.6 (6 -CH_2O-), 69.5 (2 -$\underline{C}H_2$-CH_2-OSO_2-O-), 61.5 (2 -$\underline{C}H_2$-OSO_2-O-).

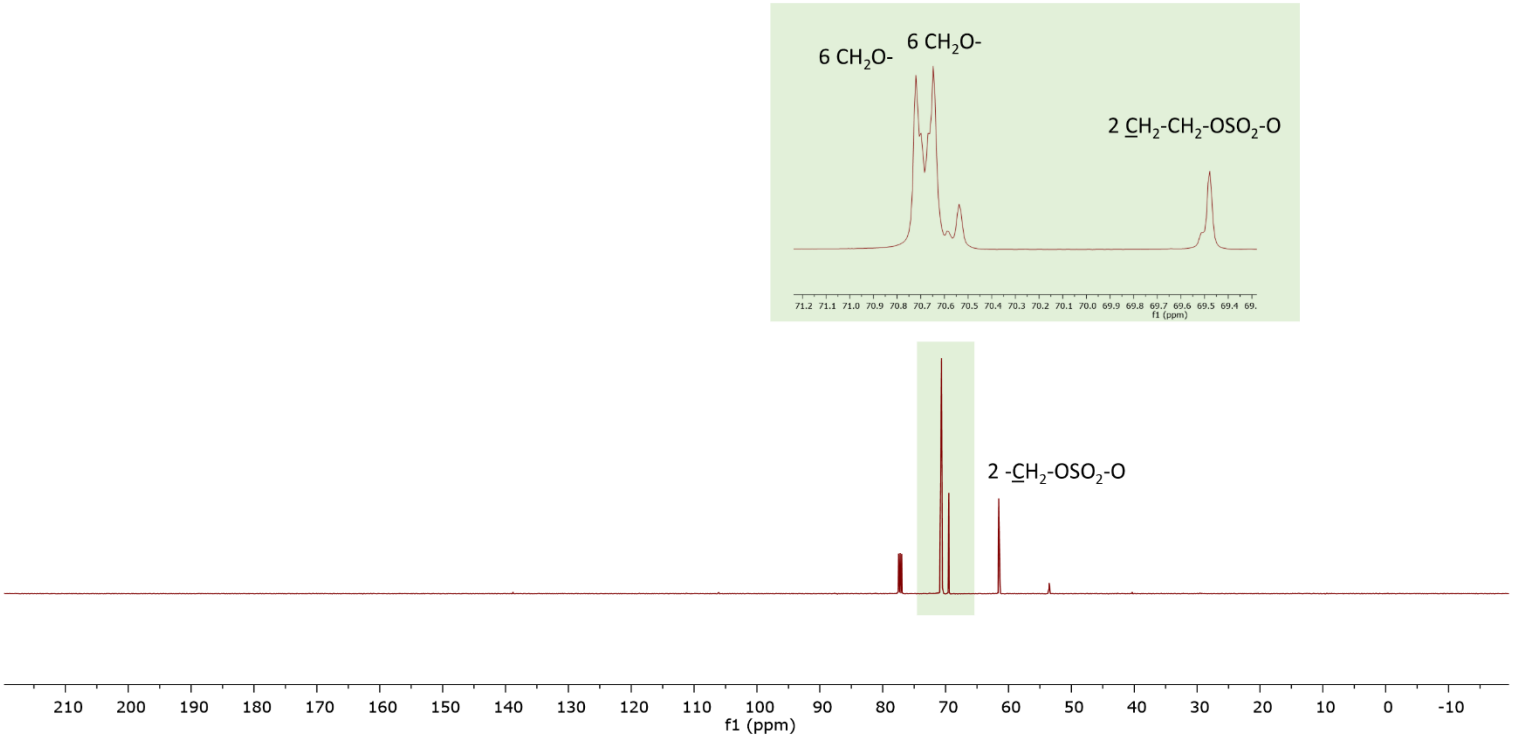

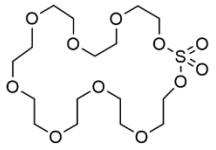

6

^{1}H NMR (500MHz, $CDCl_3$): δ 4.25 (t, 4H, *J*=4.61Hz, 2 -C$\underline{H_2}$-OSO_2-O-), 3.62 (t, 4H, *J*=4.47Hz, 2 -C$\underline{H_2}$-CH_2-OSO_2-O-), 3.52-3.36 (m, 24H, 12 OCH_2).

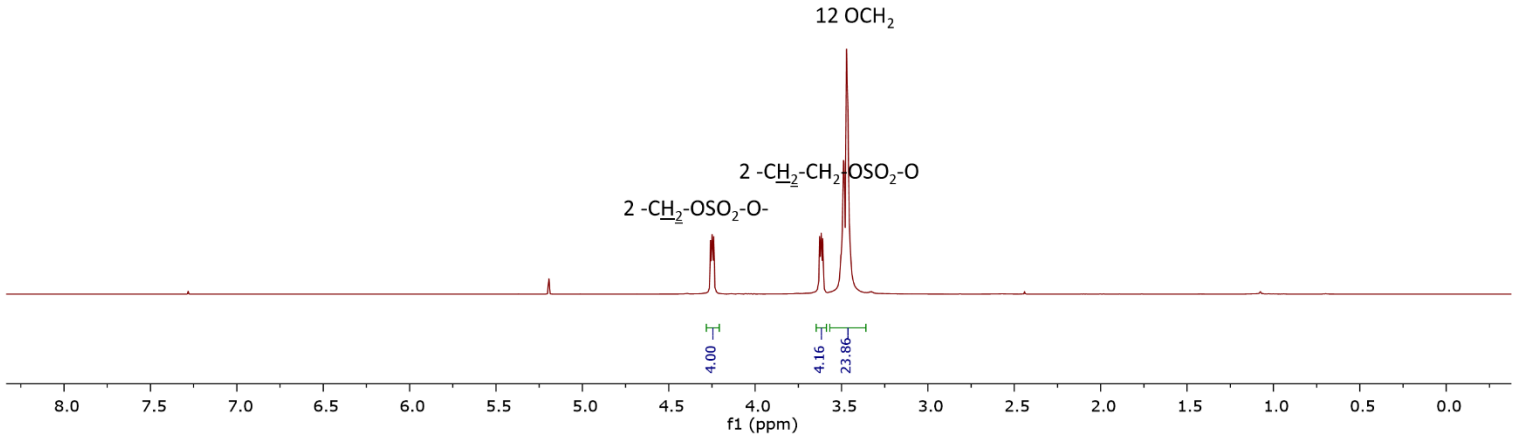

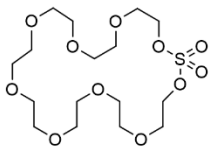

6

^{13}C NMR (125MHz, $CDCl_3$): δ 72.1 (2 -$\underline{C}H_2$-CH_2-OSO_2-O-), 70.5 (9 CH_2O-), 70.4 (3 CH_2O-), 68.1 (2 -$\underline{C}H_2$-OSO_2-O-).

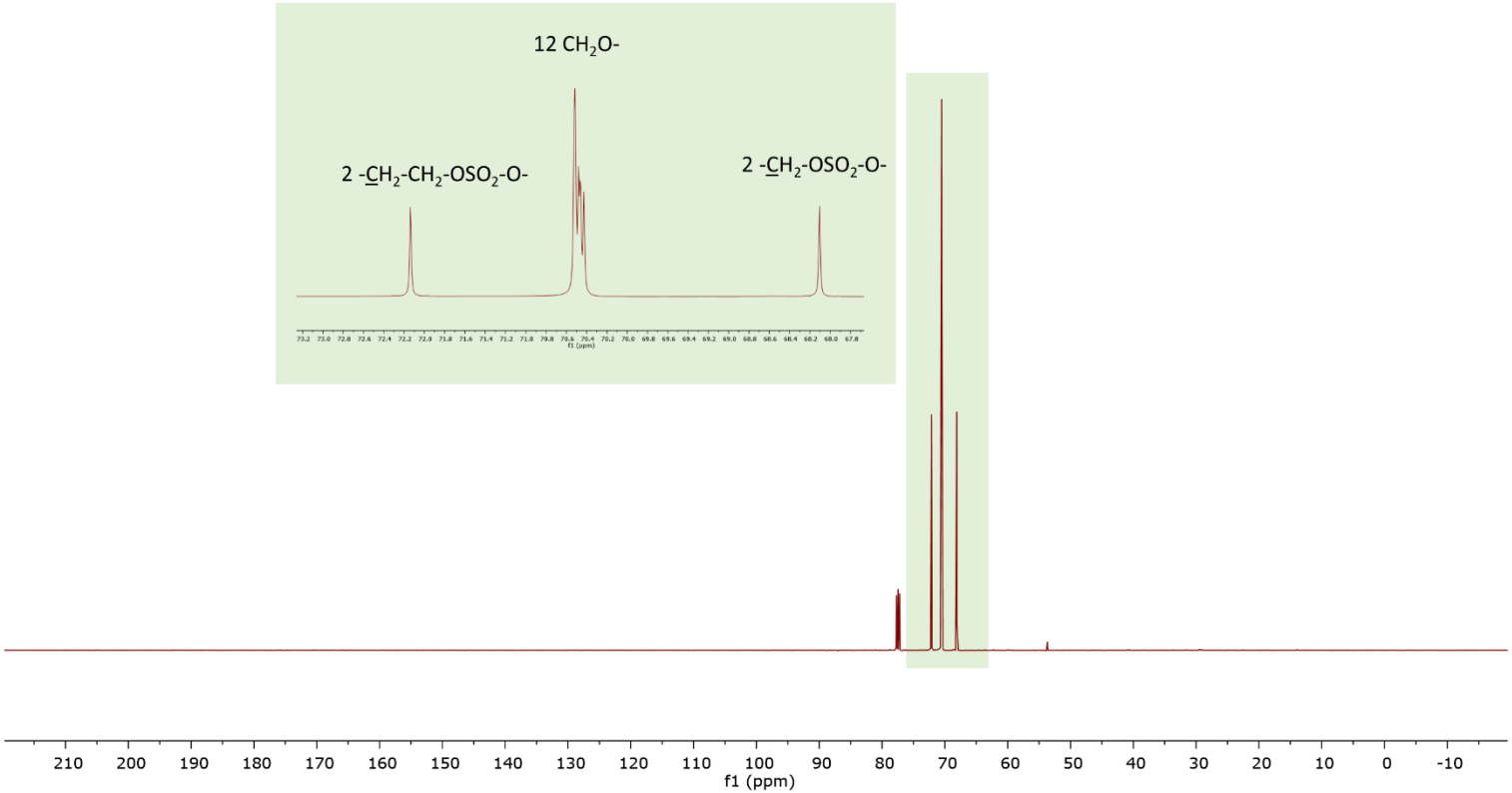

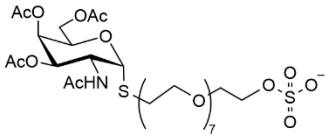

7

^{1}H NMR (500MHz, $CDCl_3$): δ 6.23 (d, 1H, $J_{NH,2}$=8.23Hz, NH-COOH-CH_3), 5.62 (d, 1H, $J_{1,2}$=5.24Hz, H-1), 5.42 (s, 1H, H-4), 5.07 (dd, 1H, $J_{3,2}$=11.70Hz, $J_{3,4}$=2.84Hz, H-3), 4.78-4.71 (m, 1H, H-2), 4.56 (t, 1H, $J_{5,6a}$=$J_{5,6b}$=6.40Hz, H-5), 4.23 (t, 2H, J=3.83Hz, CH_2-OSO_3-), 4.17-4.11 (m, 1H, H-6a), 4.11-4.05 (m, 1H, H-6b), 3.77-3.47 (m, 28H, 14 OCH_2), 2.91-2.73 (m, 2H, S-CH_2-CH_2-), 2.16 (s, 3H, -COO-CH_3) , 2.06 (s, 3H, -COO-CH_3), 2.01 (s, 3H, -COO-CH_3), 2.00 (s, 3H, -COO-CH_3).

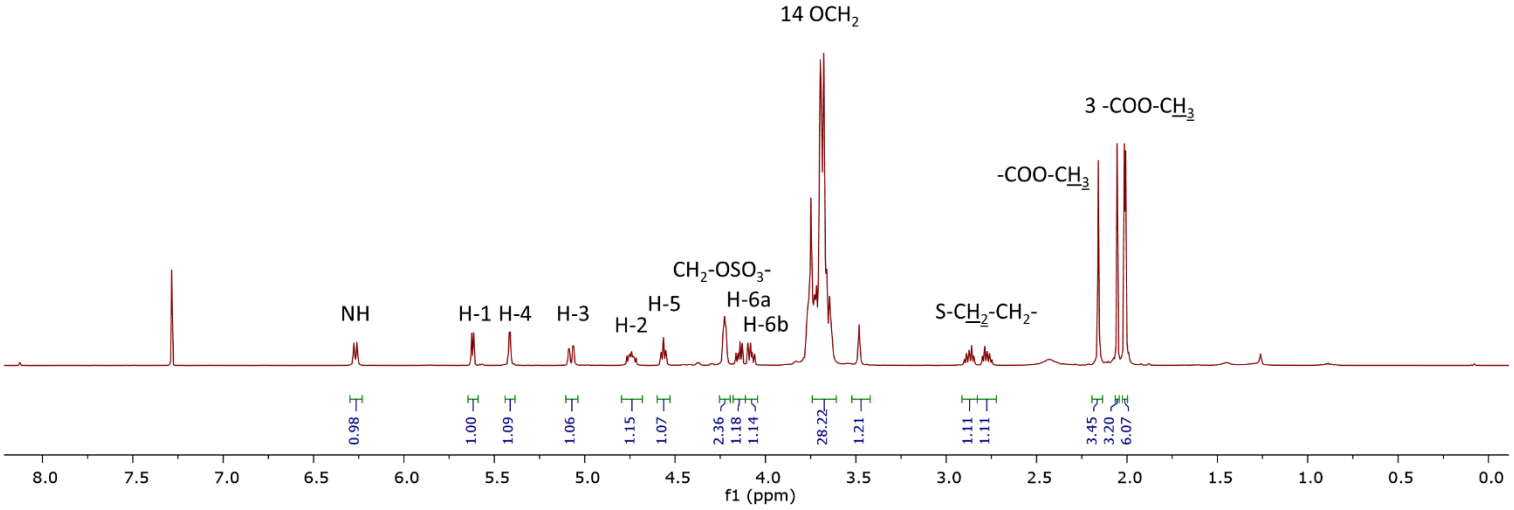

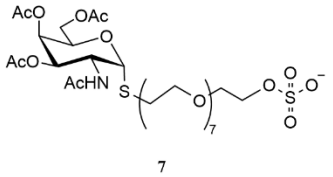

7

^{13}C NMR (125MHz, $CDCl_3$): δ 171.0 (CO), 170.7 (CO), 170.4 (CO), 170.3 (CO), 84.9 (C1), 70.3 (-CH_2-), 70.1 (-CH_2-), 70.0 (-CH_2-), 69.9 (-CH_2-), 69.9 (-CH_2-), 69.7 (-CH_2-), 69.6 (-CH_2-), 69.6 (-CH_2-), 69.6 (-CH_2-), 69.5 (-CH_2-), 69.5 (-CH_2-), 69.4 (-CH_2-), 69.3 (-CH_2-), 68.4 (C3), 67.3 (C4), 67.1 (C5), 66.4 (-CH_2-), 61.2 (C6), 48.3 (C2), 30.2 (-CH_2-), 23.2 (CH_3), 20.8 (CH_3), 20.7 (CH_3), 20.7 (CH_3).

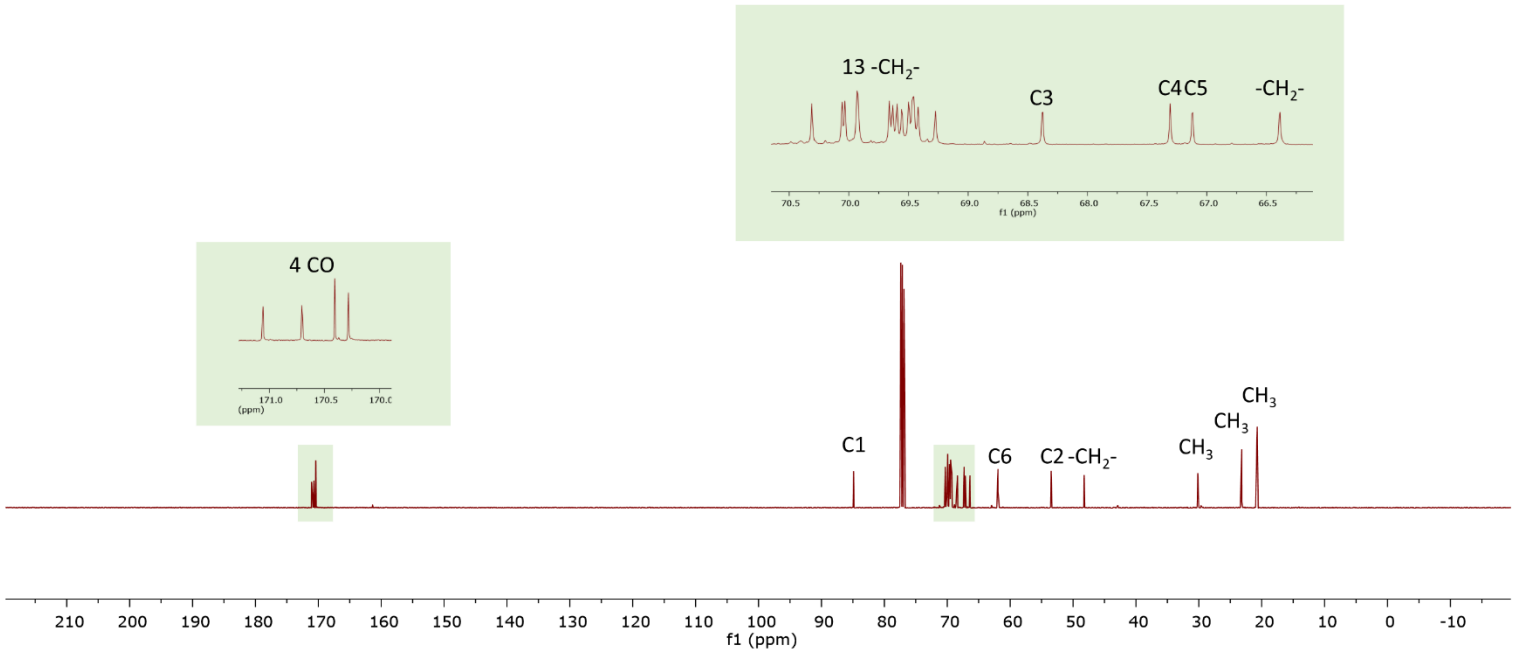

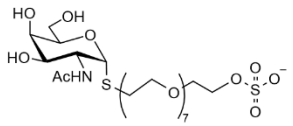

8

^{1}H NMR (500MHz, MeOD): δ 5.63 (d, 1H, $J_{1,2}$=5.39Hz, H-1), 4.45-4.39 (m, 1H, H-2), 4.22-4.13 (m, 3H, H-5, SO_4-C<u>H$_2$</u>-), 3.93 (d, 1H, $J_{4,3}$=3.29Hz, H-4), 3.80-3.63 (m, 31H, H-6, H-3, 14 OCH_2), 2.92-2.68 (m, 2H, S-C<u>H$_2$</u>-CH_2-), 2.00 (s, 3H, -COO-C<u>H$_3$</u>).

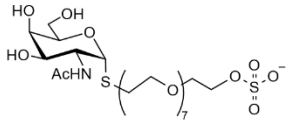

8

^{13}C NMR (125MHz, MeOD): δ 172.5 (CO), 84.3 (C1), 71.6 (-CH_2-OSO_3^-), 70.4 (-CH_2-), 69.7 (-CH_2-), 69.7 (-CH_2-), 69.6 (-CH_2-), 69.6 (-CH_2-), 69.6 (-CH_2-), 69.5 (-CH_2-), 69.5 (-CH_2-), 69.5 (-CH_2-), 69.5 (-CH_2-), 69.4 (-CH_2-), 69.4 (-CH_2-), 69.4 (-CH_2-), 69.3 (-CH_2-), 68.9 (C4), 67.9 (C3), 66.8 (C5), 61.4 (C6), 50.5 (C2), 29.2 (-S-CH_2-), 21.3 (CH_3).